Research Article

For reprint orders, please contact: reprints@futuremedicine.com

Nanomedicine

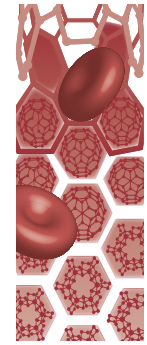

Stimuli-sensitive thiolated hyaluronic acid based nanofibers: synthesis, preclinical safety and *in vitro* anti-HIV activity

Aim: To develop a seminal enzyme bioresponsive, mucoadhesive nanofibers (NFs) as safe and effective nanocarriers for the prevention of HIV vaginal transmission. **Methods:** A novel thiolated hyaluronic acid (HA-SH) polymer was synthesized to fabricate tenofovir (TFV)-loaded electrospun NFs (HA-SH-NFs) and characterized *in vitro*/*in vivo*. **Results:** A triggered drug release (87% w/w) from the engineered HA-SH-NFs (mean diameter ~75 nm) occured within 1 h under the influence of seminal hyaluronidase enzyme. HA-SH-NFs were noncytotoxic, induced no damage on the C57BL/6 mice genital-tract and other organs. No significant CD45 cell-infiltration and changes in cytokines level in cervicovaginal tissues were observed. HA-SH-NFs significantly enhanced both TFV retention and bioavailability in vaginal tissue compared with the 1% TFV-gel. The anti-HIV activity of TFV (on pseudotyped virus followed by luciferase assay) was not adversely affected by the electrospinning process. **Conclusion:** HA-SH-NFs developed in this study could potentially serve as a safe nanotemplate for topical intravaginal delivery of HIV/AIDS microbicides.

First draft submitted: 11 March 2016; Accepted for publication: 19 August 2016; Published online: 27 October 2016

Keywords: anti-HIV activity • electrospinning • HIV vaginal transmission • nanofibers • preclinical safety • tenofovir • thiolated hyaluronic acid • topical microbicide • vaginal delivery

Vivek Agrahari[†,1], Jianing Meng[†,1], Miezan JM Ezoulin[‡,1], Ibrahima Youm[‡,1,2,§], Daniel C Dim[3], Agostino Molteni[3], Wei-Ting Hung[4], Lane K Christenson[4] & Bi-Botti C Youan*[,1]

[1]Laboratory of Future Nanomedicines & Theoretical Chronopharmaceutics, Division of Pharmaceutical Sciences, School of Pharmacy, University of Missouri-Kansas City, Kansas City, MO 64108, USA

[2]Hough Ear Institute, Oklahoma City, OK 73112, USA

[3]School of Medicine, University of Missouri-Kansas City School of Medicine, Kansas City, MO 64108, USA

[4]Department of Molecular & Integrative Physiology, University of Kansas Medical Center, Kansas City, KS 66160, USA

*Author for correspondence:
Tel.: +1 816 235 2410
Fax: +1 816 235 5779
youanb@umkc.edu

[†]Authors contributed equally

[‡]Authors contributed equally

[§]Current affiliation

According to the recent report of the global AIDS epidemic, nearly 37 million people are currently living with HIV/AIDS infections. Since the epidemic began in the early 1980s, more than 30 million people have died of HIV-related infections. With 2 million new infections and 1.2 million deaths in 2014–2015, AIDS still remains the deadliest epidemic of our time [1]. The female-controlled prophylactic methods using microbicides are the major focus among HIV prevention strategies. Topical microbicides are agents applied within the vagina or rectum to prevent the transmission of sexually transmitted diseases including HIV infections [2,3]. The success of vaginal delivery systems depends on the locally prolonged residence time of drug-containing formulations [4]. Mucoadhesive polymers are widely used in vaginal delivery due to their prolonged contact with the adsorption site [5]. These polymers interact with mucus by van der Waals, hydrophobic, electrostatic and hydrogen bond interactions. Consequently, through the mucoadhesion process the therapeutic efficacy of drugs can be efficiently improved [5].

In recent years, hyaluronic acid (HA) has been used widely in drug delivery applications due to its excellent physicochemical properties [6–9]. It is a naturally occurring, nonimmunogenic, hydrophilic polysaccharide made of repeating disaccharide units of D-glucuronic acid (GlcA) and *N*-acetyl-D-glucosamine (GlcNAc), linked through β(1–4) and β(1–3) glycoside bonds [10,11]. However, HA is characterized

Future Medicine part of fsg

by its weak mucoadhesive properties due to the presence of carboxylate (-COOH) groups on its GlcA units which creates weak hydrogen bonding with mucin [12]. In contrast, functionalized polymers bearing sulfhydryl (SH) groups on their backbone are capable of forming strong interactions with cysteine subunits of mucin [13].

Recently, a lot of the emphasis has been put on the microbicide vaginal gel formulations. However, such gel systems suffer from several disadvantages such as their limitation of encapsulating hydrophobic microbicides, the low retention time requires a high dosing frequency, poor acceptability and adherence [14]. Nanomedicine approaches play an important role in vaginal and rectal microbicide delivery [15]. Nowadays, electrospun nanofibers (NFs) are extensively studied in drug delivery applications [16,17]. NFs formulations offer various potential advantages in vaginal drug delivery such as high drug loading efficiency, flexibility to be formulated in various shapes and no leakage or messiness [18,19]. The added advantages of electrospun fibers include high surface-to-volume ratio and porosity [19]. These benefits make the drug-loaded NFs an attractive platforms for the formulations of therapeutic molecules. Furthermore, the encapsulation of labile molecules in polymeric nanocarrier systems such as NFs can enhance their stability against a harsh acidic vaginal environment and presence of enzymes such as proteases, hydrolases and phosphatases.

Tenofovir (TFV) is a nucleotide reverse-transcriptase inhibitor under the category of antiretroviral drugs. It is a weakly acidic, water-soluble drug with a molecular weight (MW) of 287.213 Da [20]. The effectiveness and safety of TFV as an anti-HIV vaginal microbicide has been demonstrated [14]. Recently, several topical TFV formulations, including vaginal gel [21], vaginal ring [22], solid lipid nanoparticles (NPs) [23], mucoadhesive chitosan NPs [24,25], pH responsive NPs [26], pH responsive microspheres [27] and enzyme-sensitive NPs [2], were developed. However, there are few papers related to the use of electrospun NFs approach in HIV vaginal transmission prevention strategies [28,29]. Based on the effectiveness of TFV against HIV, it was used as the model HIV microbicide drug in this study.

It is known that HA is hydrolysable following treatment with hyaluronidase (HAase) enzyme [30], which is abundant in human seminal fluid [31–33] as well as other body fluids and tissues [6]. The mechanism of HA degradation under several conditions has already been reviewed [34]. Since, human semen is a potential carrier of HIV virus during male to female intercourse [35], designing a semen-triggered delivery system would have the potential to locally inactivate or kill the HIV virus prior to the penetration of the vaginal mucosa and systemic exposure. Based on the foregoing facts, in this study, it was hypothesized that bioresponsive and mucoadhesive hyaluronic acid-nanofibers (HA-SH-NFs) can be topically safe platforms for an effective prevention of HIV virus transmission through the vaginal mucosa. On exposure to seminal HAase enzyme, the HA-based nanocarrier would provide a triggered release of microbicide drug (TFV) as illustrated in Figure 1. To test this hypothesis, sulfhydryl (-SH) group modified thiolated HA (HA-SH) derivatives were synthesized and characterized. Thiolated HA derivatives were then used to engineer the HA-SH based NFs and tested *in vitro* and *in vivo* as described below.

Materials & methods

Chemicals

TFV was purchased from Beijing Zhongshuo Pharmaceutical Technology Development Co. Ltd. (Beijing, China). Hyaluronic acid sodium salt was kindly provided by Mr. Jack Liu (Zhenjiang DongYuan Biotech Co., Ltd., Jiangsu, China). HAase from bovine testes with a specified activity of 810 U/mg, purified type II mucin from porcine stomach, 5,5′-Dithio-bis-(2-nitrobenzoic acid) (DTNB), poly (ethylene oxide) (PEO: MW of 400 kDa), cysteine hydrochloride, ethylene sulfide, Dithiothreitol and deuterium oxide (D_2O) were from Sigma-Aldrich (MO, USA).

The human vaginal epithelial (VK2/E6E7), endocervical epithelial (End1/E6E7) cell lines and *Lactobacillus crispatus* bacteria were from the American Type Culture Collection (ATCC, VA, USA). The CellTiter 96® AQueous One Solution Proliferation assay kit with (3-[4,5-dimethylthiazol-2-yl]-5-[3-carboxymethoxyphenyl]-2-[4-sulfophenyl]-2Htetrazolium, inner salt; MTS) reagent and CytoTox-ONE™, lactate dehydrogenase (LDH) cytotoxicity assay kit were from Promega (WI, USA). Deionized water for all the experiments was obtained through a Millipore Milli Q water purification system (Millipore Corp., MA, USA). All other chemicals were of analytical grades and used as obtained from the suppliers. The pH was measured using a SevenEasy pH meter (Mettler Toledo, Schwerzenbach, Switzerland) under ambient temperature conditions (22–24°C).

Synthesis & characterization of thiolated hyaluronic acid (HA-SH) derivative

The sulfhydryl (-SH) group modified thiolated HA derivatives (HA-SH) were synthesized using the nucleophilic opening reaction of ethylene sulfide [36] as shown in Figure 2. Briefly, an aqueous solution of HA (0.5% w/v) was prepared using Milli-Q water and stirred for 2 h to make a homogeneous solution.

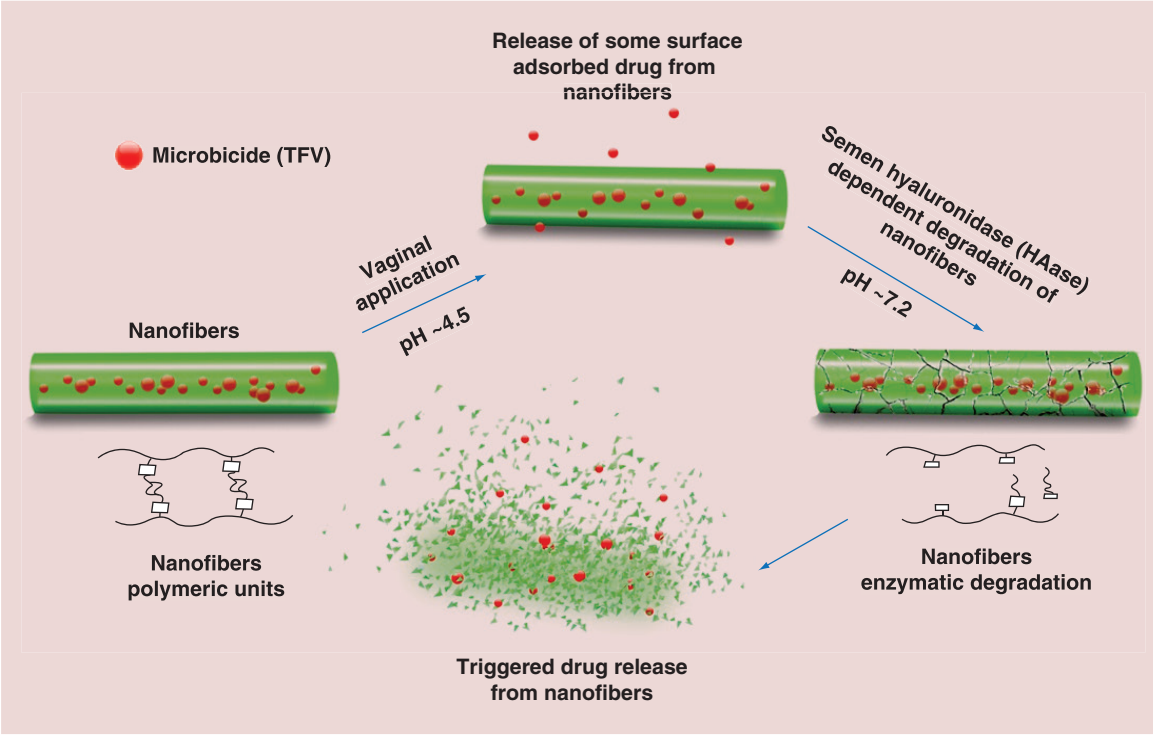

Figure 1. Mechanism of HIV microbicide drug release from bioresponsive nanofibers under the influence of human seminal fluid hyaluronidase (HAase) enzyme.
TFV: Tenofovir.

The pH of the solution was raised to 9.5 using sodium hydroxide (NaOH) solution. A fivefold molar excess of the ethylene sulfide was added drop-wise to the above solution and the reaction mixture was stirred for 24 h at room temperature. To separate the precipitate generated due to the oligomerization of ethylene sulfide, the solution was vacuum filtered. To the clear filtrate, a fivefold molar excess of dithiothreitol was added to reduce the disulfide (S–S) bonds. The pH of the solution was raised to 8.5 using NaOH solution and mixture was further stirred for 24 h at room temperature. The pH of the reaction mixture was then acidified to 3.5 using the hydrochloric acid (HCl) solution. To purify the final HA-SH product, acidified solution was dialyzed against diluted HCl solution (pH 3.5) for 24 h using a dialysis membrane (Spectra/Por Float-A-Lyzer G2, MWCO: 8–10 kDa) supplied from Spectrum Laboratories Inc. (Rancho Dominguez, CA, USA) with media changes at every 8 h. The final product was then lyophilized (Labconco Corp., MO, USA) and stored at 2–8°C until further analysis.

The HA-SH derivatives were thoroughly characterized for their molecular weight by size exclusion chromatography (SEC), chemical structure by proton nuclear magnetic resonance (^{1}H-NMR) and Fourier transform infrared (FT-IR) spectroscopy, -SH group quantification using Ellman's method [37], and crystallography using powder x-ray diffraction (PXRD) analysis. The detailed experimental conditions of all these assays are in the supplementary file.

Fabrication of HA-SH-based NFs using electrospinning method

In the electrospinning process, a polymer solution was injected through a needle by electrostatic repulsive forces on a grounded collector (Figure 3A). Native HA or HA-SH polymer solutions alone were difficult to processed by electrospinning into NFs due to their high viscosity and enormous water affinity [38]. To improve the electrospinnability of HA, PEO (MW 400 kDa), a well-known fiber forming polymer [39,40] was used as a core material. The potential use of PEO as a fiber forming polymer and for other biomedical applications has attracted a great attention due to its water-soluble, biodegradable and biocompatible characteristics [41]. Preliminary experiments were performed to get the optimal conditions for the electrospinning process. The electrospinning process parameters such as feeding rate, applied voltage and needle tip-to-collector distance were optimized. However, the formulation variables were the concentration, MW and solubility of the polymers [42,43].

To formulate the HA-SH-NFs, the aqueous solutions of HA-SH (20 mg/ml) and PEO (30 mg/ml)

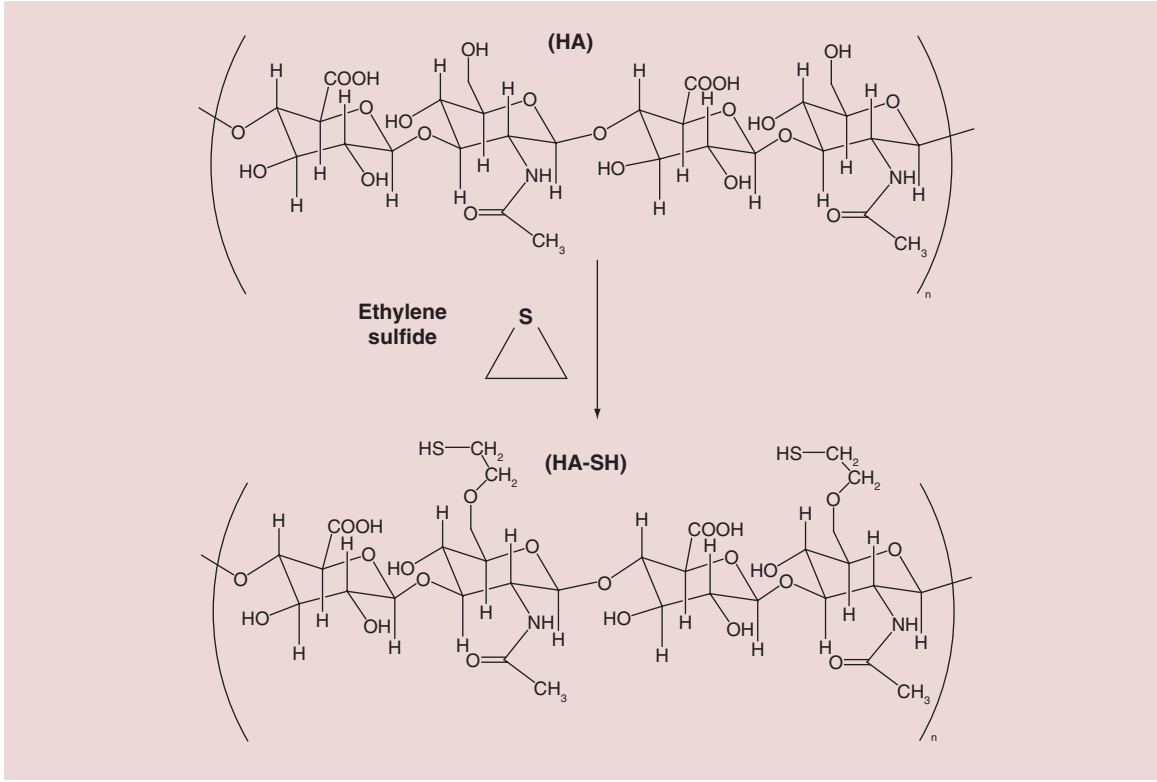

Figure 2. Synthetic scheme of thiolated derivatives of hyaluronic acid.
HA-SH: Thiolated hyaluronic acid.

were prepared at room temperature by stirring for 2 h, and 24 h, respectively. An electrospun system with a coaxial nozzle (NaBond Technologies Co., Ltd., Hong Kong, China) was used for HA-SH-NFs production. The inner core (PEO) and outer shell (HA-SH) solutions were placed separately in two glass syringes (Becton, Dickinson and Company, NJ, USA). For the preparation of drug (TFV) loaded HA-SH-NFs, free TFV (10 mg/ml) was mixed with the PEO solution and used as core material. Two syringe pumps (Cole-Parmer Instrument Company, IL, USA) were used to provide a constant feeding rate (0.02 ml/h) of each solutions. A voltage of 15 kV was applied in the electrospinning process using a high voltage power supply (Gamma High Voltage Research, Inc., FL, USA). The distance from electrospinning syringe needle tip-to-collector was kept constant at 10 cm. HA-SH-NFs were collected onto an aluminum foil connected to the ground. The NFs were vacuum dried at room temperature for 48 h and stored in a vacuum desiccator until further use.

Physicochemical characterization of HA-SH-NFs

The developed HA-SH-NFs were characterized for several physicochemical parameters such as surface morphology, size distribution, mucoadhesive property and *in vitro* drug release profile.

Surface morphology & size distribution analyses

Surface morphology of HA-SH-NFs was analyzed by scanning electron microscopy (SEM) method. Briefly, a small amount of the NFs was put onto a grid. The membrane was mounted on a 1/200 SEM stubs with double-sticky carbon tape. Samples were then sputter coated with 20 nm thickness of gold and visualized under a Philips SEM 515 microscope (Eindhoven, The Netherlands) and observations were performed at an accelerating voltage of 5 kV. The diameter of individual NFs was analyzed using Image Pro® Plus software (Image-Pro®Plus 6.0, Media Cybernetics, MD, USA). At least 100 NFs were counted per group. The histogram and distribution curve were generated by IBM® SPSS® Statistics software Version 23 (IBM Corp., NY, USA).

Drug loading determination

To determine the drug loading, NFs at the concentration of 1 mg/ml were dispersed in water under constant shaking at 100 r.p.m. for 48 h to allow complete dissolution of the PEO core and vortexed for 5 min. The sample was centrifuged at 19,500 × *g* for 30 min and the supernatant was analyzed by liquid chromatography-mass spectroscopy (LC-MS) assay of TFV [44]. The drug loading was calculated using Equation 1:

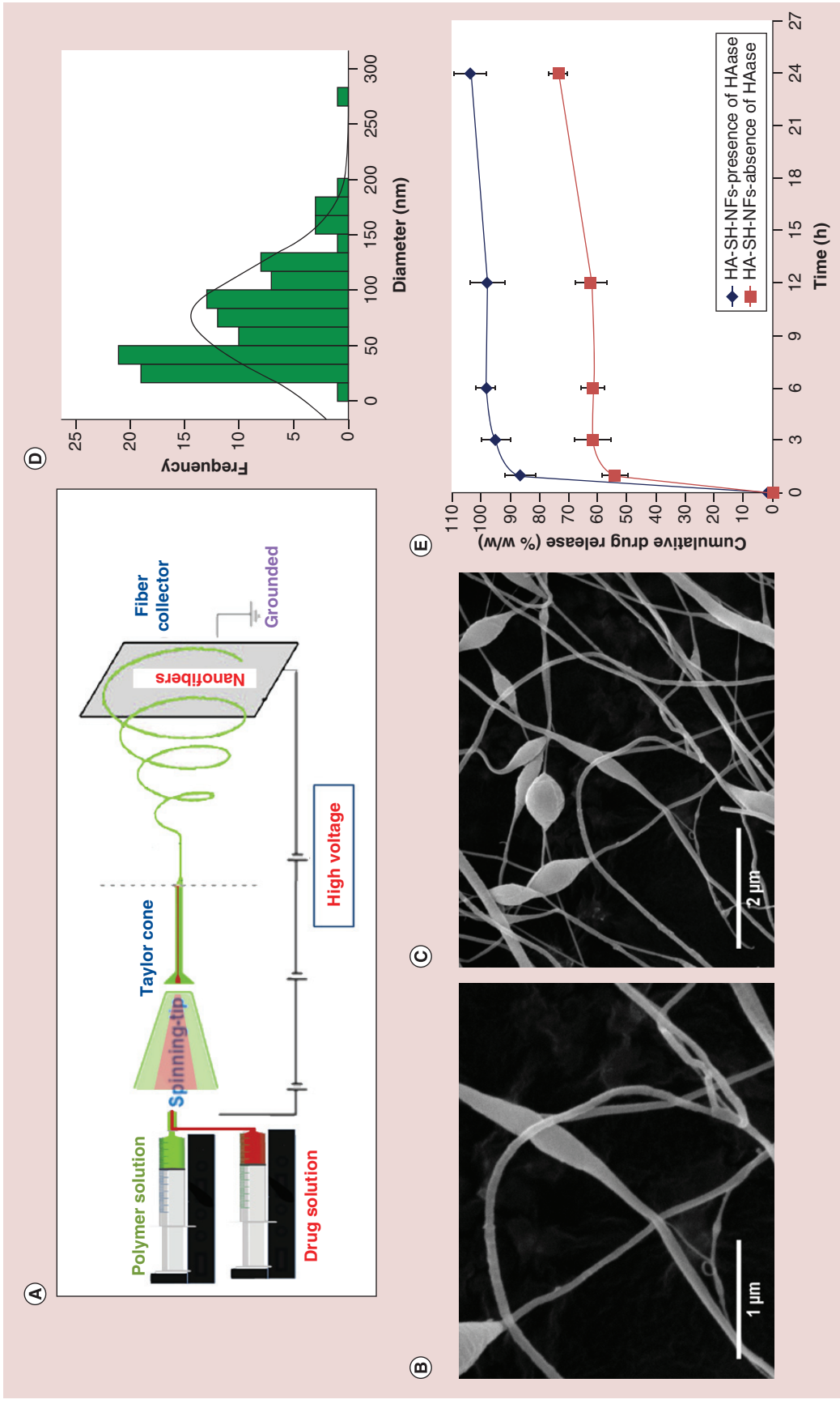

Figure 3. Nanofiber fabrication, characterization and drug release profile. **(A)** NF fabrication using electrospinning method. Surface morphology of: **(B)** HA-SH-NFs; scale bar, 1 µm. **(C)** HA-SH-NFs with beads formation; scale bar, 2 µm. **(D)** Size distribution analysis of HA-SH-NFs determined by image analysis software and averaged using at least 100 measurements per group. **(E)** Percent cumulative drug release (%w/w) profile of tenofovir-loaded HA-SH-NFs either in the presence or absence of HAase enzyme. Results are given as mean ± SD, n = 3.
NF: Nanofiber.

$$\text{Drug loading (\%)} = \frac{\text{Total amount of TFV in mg}}{\text{Total amout of NFs in mg}} \times 100$$

In vitro mucoadhesion analysis

In vitro mucoadhesion analysis of HA-SH-NFs was performed using mucin interaction [45,46] and ellipsometer measurements [47–49]. Mucin interaction method was used to study the mucin-NFs interactions in solution form and ellipsometer measurements were used to study the interactions between HA-SH-NFs and the mucin-coated silica surfaces.

Mucoadhesion assessment by mucin interaction method

Mucin interaction analysis was performed using native HA, and HA-SH-NFs at the concentration of 10 mg/ml in phosphate buffer saline (PBS) (pH 7.4), vaginal fluid simulant (VFS) (pH 4.2) and in water (with 10 mM sodium chloride: NaCl), prepared accordingly [50,51]. The mucin at the concentration of 1.5% w/v [46] was used in the analysis. The polymer samples were incubated for 0, 3, 6 and 24 h at 37°C and 60 r.p.m. with or without mucin. The size and zeta (ζ) potential values were analyzed by Laser Doppler Velocimetry and Phase Analysis Light Scattering methods using Zetasizer Nano ZS (Malvern Instruments Ltd., Worcestershire, UK) at 25°C. The instrument was calibrated by using nanosphere™ of PMD (59.0 ± 2.5 nm) and ζ potential standards (-68.0 ± 6.8 mV).

Mucoadhesion assessment by ellipsometer measurements

Ellipsometer is the study of adsorbed mass on a polymer surface [49]. The adsorption of mucin and polymers on methylated silicon wafer surface was studied using an alpha-SE® ellipsometer (J.A. Woollam Co. Inc., NE, USA) at a single angle of incidence. The acquisition and analysis of ellipsometer data was performed using CompleteEASE® software version 5.03 (J.A. Woollam Co. Inc., NE, USA). Two inch-diameter silicon wafers (WRS Materials, CA, USA) were hydrophobized (methylated) to enhance their interactions with proteins [52,53] as previously described [54]. Briefly, silicon wafers with thermal oxide layer of 30 ± 3 nm (n = 3) were dipped into a solution of trimethylchlorosilane in ethanol (1:5 v/v ratios) for 2 h. Afterwards, the wafers were rinsed with water followed by ethanol (three-times each) and stored in ethanol prior to use. Immediately before use, wafers were rinsed with water, blown dry using nitrogen gas, dipped in a mucin solution (1.5% w/v) and incubated for 15 h at 37°C followed by sequential washing with ethanol and water. The native HA and HA-SH-NFs solutions at the concentration of 10 mg/ml in PBS (pH 7.4) were added on methylated wafers and analyzed by ellipsometer at 30, 60 and 120 min.

A change in polarization was measured after light was reflected from the wafer surfaces. The data were represented as two values: Psi (Ψ, amplitude ratio) and Delta (Δ, phase difference) [55]. Interference occurs as light recombined after traveling different paths through the thin film. The thickness (d) measured was used to calculate the adsorbed mass (m in µg/cm^2) using Equation 2:

$$\text{Adsorbed mass (m)} = \frac{d\,(n - n_0)}{dn/dc}$$

Where, n and n_0 are the refractive index of the sample and the ambient environment, respectively, dn/dc is the refractive index increment as a function of bulk concentration (0.165 ml/g) of mucin [56].

In vitro drug release analysis

In vitro drug release analysis of HA-SH-NFs in the presence or absence of HAase enzyme was performed using dialysis method. An amount of HAase (1.08 U) similar to that is normally present in human ejaculate containing 100 million sperms/ml was used in the drug release analysis considering the average volume of human ejaculate of 3 ml [31]. Briefly, the drug loaded HA-SH-NFs were transferred to a dialysis bag (MWCO, 3.5–5 kDa) containing the simulant mixture (pH 7.2) of the VFS (pH 4.2) and seminal fluid simulant (SFS: pH 7.8) and placed inside a dialysis tube containing the release medium (PBS, pH 7.2). These VFS and SFS buffers were prepared according to the previous reports [50,51]. The whole system was then placed in a thermostatic shaking water bath (BS-06, Lab Companion, Seoul, Korea) at 37°C with constant agitation at 60 r.p.m. Aliquots of samples (100 µl) were taken at 0, 1, 3, 6, 12, 24 h from the release medium. Simultaneously, an equivalent volume of the fresh release medium was added at the same rate to maintain the sink conditions. The amount of drug released from HA-SH-NFs was quantified using the LC-MS assay of TFV [44].

Drug release kinetics of TFV loaded HA-SH-NFs was analyzed by various kinetic models [2,57] using the previously described add-in DDSolver program [58]. The kinetic models used were zero-order, first-order, Higuchi, Korsmeyer-Peppas, Hixson-Crowell, Weibull and Quadratic models [58]. The criteria for selecting the most appropriate model were based on the correlation coefficient (R), the coefficient of determination, (R^2) and the Akaike information criterion (AIC) [58].

In vitro cytotoxicity assays of HA-SH-NFs

Cytotoxicity assays on vaginal epithelial cells

The cytotoxic effects of HA-SH-NFs in the concentration range of 1–1000 µg/ml were tested on the viability (MTS assay) and membrane integrity (LDH assay) of VK2/E6E7 and End1/E6E7 cells using published protocols [2]. To perform the MTS assay, cells were seeded to 96-well plates in a keratinocyte-serum free medium and grown until 80% confluence. The cell culture medium was replaced with 100 µl of native HA or HA-SH-NF samples in the concentration range of 1–1000 µg/ml. Samples were kept in contact with the cells for 48 h. The amount of formazan product was determined by adding 20 µl of MTS reagent to the culture wells. The 96-well well plates were incubated for 4 h at 37°C in a humidified, 5% CO_2 atmosphere and the absorbance was measured at 490 nm using a DTX 800 multimode microplate reader (Beckman Coulter, CA, USA). The medium and 1% Triton X was used as negative and positive controls, respectively. The percent (%) cell viability was determined using Equation 3:

$$\text{Viability (\%)} = \frac{\text{ABS (test)}}{\text{ABS (control)}} \times 100$$

Where *ABS* (*test*) and *ABS* (*control*) represented the absorbance of the amount of formazan product generated in viable cells.

To perform the LDH assay, the cells were incubated with 100 µl medium containing the samples of native HA and HA-SH-NFs in the concentration range of 1–1000 µg/ml. The 96-well well plates were incubated at 37°C for 48 h and equilibrated to room temperature for 30 min. One hundred microliters of CytoTox-One reagent was added in each well and vortexed for 30 s. The plates were incubated at room temperature for 10 min. Fifty microliters of stop solution from Promega was added in each well and the plates were shaken for 10 s. The fluorescence intensity was measured at the excitation/emission wavelengths of 560 nm/590 nm, respectively, using the above microplate reader. The percent (%) cytotoxicity was determined using Equation 4:

$$\text{Cytotoxicity (\%)} = \frac{\text{Experimental} - \text{Background}}{\text{Positive control} - \text{Background}} \times 100$$

Where experimental, background and positive control represented the fluorescence intensity of the wells with and without sample treatment, and with 1% Triton X treatment, respectively.

Lactobacillus crispatus viability assay

A microbicide formulation should not disturb the normal *Lactobacillus* vaginal microflora since this can enhance the risk of HIV transmission through cervicovaginal (CV) mucosa [59]. In this study, *L. crispatus* bacteria was used as representative species since it is one of the most common vaginal *Lactobacillus* [60]. *L. crispatus* was grown in ATCC medium 416 *Lactobacilli* MRS broths (BD Biosciences, NJ, USA) at 37°C. The viability assay was performed using *Lactobacillus* viability assay [25]. Briefly, the bacteria density was adjusted to an OD_{670} of 0.06, corresponding to 0.5 McFarland Standard or 10^8 CFU/ml. The *L. crispatus* bacteria was seeded in a 96-well plate at a volume of 100 µl and incubated with 100 µl of the sample suspension for 48 h at 37°C. The 96-well well plates were treated with 10 µg/ml of commercially available penicillin-streptomycin solution (positive control) from Invitrogen (CA, USA). After the incubation, 20 µl MTS reagent was added to each well and the absorbance was measured at 490 nm to express the viability using Equation 3.

In vivo evaluation on animal (mice) model

Female C57BL/6 mice with an average body weight of 20 g at 8–12 weeks old from Jackson Laboratories (Harbor, ME) were used for the *in vivo* evaluations of HA-SH-NFs. All mice were housed (no more than 5 per cage) under a 12 h light: dark regime in the UMKC Laboratory Animal Resource Center facility which is a fully AAALAC (the Association for Assessment and Accreditation of Laboratory Animal Care) accredited with HEPA-filtered, temperature, humidity and lighting control systems.

Vaginal cytology: mice estrous cycle stage identification

Mice were treated with 2 mg of subcutaneous medroxyprogesterone acetate (Depo-Provera®, NJ, USA) diluted in Lactated Ringer's solution at 4–5 days prior to the *in vivo* experiments. This treatment induced a diestrus-like state that is characterized by thinning of the vaginal epithelial layer and reduced inter-individual variability of vaginal histology [61]. Vaginal cytology analysis was then performed to identify the mice estrous cycle stages (proestrus, estrus, metestrus, diestrus) by visualizing the nucleated and cornified squamous epithelial cells and polymorph nuclear leukocytes [62].

Preclinical safety & toxicity evaluation

In vivo safety of HA-SH-NFs at the dose of 275 mg/kg (equivalent to the drug dose of ~46 mg/kg) upon once-daily vaginal administration up to 7 days was assessed by histological analysis of mice genital tract (vagina, cervix, uterus and ovary), rectum and other organs (rectum, spleen, lung, liver, kidney, heart, brain). The vagina was washed two-times by flush-

ing repeatedly with 50 µl of PBS with a micropipette before any treatment. To instill the samples, mice were held upward by the base of the tail and samples were administered intravaginally using a micropipette with a soft tip. Care was taken in order to minimize tissue injury or disturbance of vaginal mucus. Animals were maintained in an upward position for 1 min in order to reduce immediate vaginal leakage of samples. Mice treated with nonoxynol-9 (N-9: Conceptrol®; 4% w/v) from Revive Personal (NJ, USA) and benzalkonium chloride (BZK: 2% v/v) from Sigma-Aldrich were used as positive control groups. Mice treated with PBS were used as negative control groups.

At predetermined time points, mice were euthanized by carbon dioxide (CO_2) asphyxiation at 70% (v/v) CO_2 (30% v/v oxygen). The collected tissues were formalin fixed and embedded in paraffin following standard tissue processing procedure. Histopathologic review was performed on tissues stained with hematoxylin and eosin (H&E). Images were viewed and captured using a Nikon Labophot-2 microscope (Nikon Instruments, Inc., NY, USA) equipped with a PAXCam digital microscope camera and analyzed using PAX-it image management and analysis software (Midwest Information Systems, Inc., IL, USA).

Osmolality determination of the tested samples

Ideally, the osmolality of a microbicide formulation should not exceed 400 mOsm/Kg to minimize any risk of vaginal epithelial damage [63]. Thus, before any treatment, the osmolality of each sample was analyzed (n = 3) using a Vapor Pressure 5520 Osmometer (Wescor, Inc., UT, USA) calibrated with Opti-mole 100, 290 and 1000 mOsm/kg osmolality standards. To analyze the samples osmolality, metal forceps were used to place a single 1/8″ solute-free Whatman No.1 filter paper disc (Wescor, Inc.) in the central depression of the holder. Ten microliters of each sample was expelled onto the disc and it was ensured that the area of the disc was fully covered by the sample. The sample holder was inserted into the instrument and the osmolality measurement was performed. The digital reading of the osmolality of the each sample was recorded in mOsm/kg.

Immunoassay of cytokines secretion in mice cervicovaginal lavage & tissue samples

At predetermined time points after the sample treatments, the mouse vagina was washed two-times by flushing repeatedly with 50 µl of PBS and the cervicovaginal lavage (CVL) was collected. The CVL sample was centrifuged (1000 × *g*, 10 min, 4°C) and supernatant was collected. Mice were then euthanized by CO_2 asphyxiation and the CV tissues were collected. The CVL supernatant and the tissue samples were kept frozen at -20°C until further processing. The concentration of several cytokines including interleukins IL-1α, IL-1β, IL-6, IL-7, IFN-γ-induced protein-10 (IP-10), TNF-α and mice keratinocyte-derived chemokine (MKC) was measured. The detailed experimental conditions of the processing of mice CVL and CV tissue samples for the cytokine assays according to the manufacturer's protocol (Milliplex MAP Mouse Cytokine/Chemokine Magnetic Bead Panel, EMD Millipore Corp., MA, USA) were explained in the supplementary file.

Immunohistochemical analysis to identify the inflammatory cells in vaginal tissues

The CD45-associated protein is a lymphocyte-specific membrane protein. In the present study, the immunohistological staining for CD45-positive cells was performed since an increased lymphocytes infiltration within the vagina epithelium is indicative of vaginal inflammation. To visualize the lymphocytes, CV tissues were harvested from the treated mice. The detailed experimental condition was explained in the supplementary file.

In vitro anti-HIV activity assay of HA-SH-NFs

Generation & characterization of pseudotyped HIV virus particles

The pseudotyped HIV virus particles were generated from two plasmids, one coding for the envelope, and the other for the backbone. The glycoprotein G from Vesicular Stomatitis Virus G Protein (VSV-G) was selected as the envelope protein because it allowed the infection for a very wide range of cell types from a variety of organisms and known to provide high titers [64]. The proviral vector pNL4.3.Luc.R$^-$E$^-$, with envelop deleted and with the firefly luciferase gene was selected as the reporter plasmid [64].

The pseudotyped HIV virus particles were produced by co-transfection of HEK293T producer cells using lipofectamine 2000 (Invitrogen) assay [65,66]. Plasmids encoding VSV-G were co-transfected with luciferase expressing pNL4.3.Luc.R$^-$E$^-$ plasmid to generate VSV-G pseudotyped virus [65,66]. The viral supernatant was then harvested at 72-h post-transfection, centrifuged for 15 min at low speed (500 × *g*) to remove the cellular debris. The supernatant was filtered through a 0.45 µm pore size filter and stored in aliquots at -80°C until used for the single-cycle infection assay.

To determine the titer (number of particles/ml) and size distribution of virus particles, nanoparticle-tracking analysis (NTA) was performed using a Nanosight LM10 instrument (Nanosight, Salisbury, UK) outfit-

ted with a LM14C laser. Samples were diluted first in PBS to meet the optimal concentration between 10^5 and 10^8 particles/ml. At least 300 µl of diluted sample was needed for each analysis and was vortexed before injection into the chamber. Each video of moving particles was 60 s in duration, with a shutter speed of 30 ms and camera gain of 680. Software settings for analysis were: Detection threshold: 6, Blur: auto, Minimum expected particle size: 50 nm. A minimum of 200 completed particle tracks were completed for each video and the data was analyzed using the NTA 2.3 analytical software (Malvern Inc., Worcestershire, UK). Briefly, the NTA analysis determines the particle diffusion coefficient (D_t) by measuring the movement of the particle (Brownian motion) and then this employs the Stokes–Einstein equation (Equation 5) to determine the size distribution and virus titer in each sample [67,68].

$$D_t = \frac{TK_B}{3\pi\eta d}$$

Here, T = sample temperature, K_B = Boltzmann's constant, and η = solvent viscosity. Using D_t, the sphere-equivalent hydrodynamic diameter (d) of the virus particles was determined.

In vitro anti-HIV activity

The anti-HIV activity assay was performed using MT-4 cells since they are highly permissive to viruses [69]. Briefly, MT-4 cells at the density of 5 × 10^3 cells/ml were incubated with 25 µl of free TFV or TFV loaded HA-SH-NFs suspended in cell culture medium in a concentration range of 0.035–35 µM for 24 h prior to the virus treatment. Cells were then exposed to 25 µl of the pseudotyped virus particles at the multiplicity of infection (MOI) of 1000, 5000 and 10,000 and incubated for 48 h. MOI was the ratio of the number of pseudotyped virus particles to the number of cells being exposed. The inhibition of the pseudotyped HIV virus replication was analyzed using luciferase assay due to its high sensitivity, and robustness toward a variety of drugs and complex biological samples [70]. Briefly, after the 48 h of virus particle treatment, an equal volume of luciferase buffer and substrate (Promega) was added and plates were incubated for 10 min at 37°C in 5% CO_2. The bioluminescence was then immediately measured using a Luminometer (Promega), according to the manufacturer's directions. Wells with no cells and cells suspended in medium without TFV and HA-SH-NFs were used as positive (PC) and negative control (NC) samples, respectively. The inhibition of pseudotyped HIV virus replication was presented in terms of percentage (%) of viral load.

In vitro cytotoxicity assay of HA-SH-NFs on MT-4 cells

The *in vitro* cytotoxicity of HA-SH-NFs on MT-4 cells was analyzed up to 48 h incubation using the MTS cell viability assay. Briefly, MT-4 cells were seeded to 96-well plates in RPMI 1640 medium (Invitrogen, CA, USA) supplemented with 10% fetal bovine serum and were allowed to grow until 80% confluence was reached. The medium was replaced with 100 µl of samples suspended in culture medium at different concentrations (0.035–35 µM) and pseudotyped virus particles with MOIs of 1000, 5000 and 10,000. Samples were kept in contact with the cells for 24 h at 37°C. After the incubation, 20 µl of CellTiter 96 Aqueous One Solution Reagent (Promega) was added to each well and the absorbance was measured at 490 nm after 3 h incubation at 37°C. The absorbance was directly proportional to the number of viable cells as analyzed by using Equation 3. Cells with no treatment and those treated with 1% Triton X were considered as negative and positive controls, respectively.

Pharmacokinetics (PK) profiling of HA-SH-NFs in mice

The PK parameters of HA-SH-NFs were evaluated in C57BL/6 mice. Mice PK experiments were carried out following the appropriate protocols as described above in the *in vivo* section. TFV in 1% hydroxyethylcellulose (HEC) gel is prepared according to a previous report [14]. In this single-dose study, the C57BL/6 mice were divided randomly into two groups (n = 4). Group 1 was treated with the 1% TFV-gel whereas, group 2 was treated with HA-SH-NFs containing TFV. Twenty microliters of the 1% TFV-gel or HA-SH-NFs (equivalent to TFV dose of 8 mg/kg) was applied to the mouse vagina using a micropipette with a soft tip with minimal tissue injury or disturbance of vaginal mucus. An equivalent TFV dose of approximately 8 mg/kg was based on the effective human dose (40 mg/person) [14] converted from the body surface area normalization method for mice [71]. After the treatments, animals were maintained in an upward position for 1 min in order to reduce the immediate vaginal leakage of samples. At the predetermined time points (1, 4, 8, 24 and 72 h), mice were euthanized by CO_2 asphyxiation and the vaginal and rectal tissues were collected and stored at -80°C until further analysis.

Tissue homogenization & drug extraction

The collected vagina and rectum tissues were homogenized (10 mg of tissue in 100 µl of water) with the addition of 10 µl of 100 µg/ml of internal standard (IS: Adefovir). Tissues were homogenized using an OMNI™ Tissue Homogenizer (Omni International,

GA, USA). The tissue homogenate was then used to extract the drug using acetonitrile protein precipitation method. Samples were then centrifuged for 15 min at 14,000 r.p.m. and 4°C. The clear supernatant was transferred to another tube and speed vacuumed (Eppendorf Vacufuge™ concentrator 5301, Eppendorf North America, Inc., NY, USA) to dryness. The remaining sample was reconstituted in 100 µl of water containing 1% v/v formic acid and centrifuged for 5 min at 14,000 r.p.m. and 4°C. The supernatant was transferred to an LC auto sampler vial and 20 µl was injected to the LC-MS/MS system and analyzed. LC-MS/MS method was developed, adapting the previously published protocol [72] and carried out on a UFLC Shimadzu prominence system (Shimadzu USA manufacturing Inc., CA, USA). The LC calibration curve range of TFV was 0.005–5 µg/ml (R^2: 0.999). MS studies were performed on a 3200 QTrap mass spectrometer (Applied Biosystems Sciex, MA, USA) using multiple reaction monitoring scan in positive ion mode.

The PK parameters for vaginal and rectal tissues included: maximum observed concentration (C_{max}) and corresponding time (t_{max}); area under the concentration-time curve (AUC) between 1 and 72 h ($AUC_{1–72\ h}$) were computed using the linear trapezoidal method. The tissue PK parameters (T_{max}, C_{max} and AUC_{0-t}) were analyzed using Microsoft Excel add-in PKSolver software using noncompartmental analysis [73].

Statistical data analysis

The experimental values were generally presented as mean ± standard deviation (SD) of triplicate determinations (n = 3). All animal experimental conditions (treatments and time points) were tested in a group of at least four animals (n = 4) unless otherwise mentioned. Statistical data analysis was evaluated using Student's t-test with 95% confidence interval. A p-value < 0.05 was considered statistically significant.

Results & discussion

Characterization of thiolated HA-SH derivative

In this study, a bioresponsive, mucoadhesive, biocompatible and safe HA-SH-NFs were formulated intended for the effective prevention of HIV transmission through vaginal mucosa. To test this hypothesis, initially, a thiolated HA (HA-SH) derivative was synthesized and characterized.

^{1}H-NMR & FT-IR spectroscopy analyses

Thiol group's derivatives were generated at the primary hydroxyl group of the GlcNAc units of HA using the nucleophilic opening reaction of ethylene sulfide (Figure 2). Compared to the spectrum of HA, a peak corresponding to the methylene group attached to the former hydroxyl oxygen (-CH_2-CH_2-SH), appeared at approximately 3.8 ppm in the ^{1}H-NMR spectrum of HA-SH. The second methylene group, closer to the -SH functionality overlapped with GlcA and GlcNAc protons of HA from 3.0 to 3.8 ppm and appeared at approximately 3.65 ppm [74] (Supplementary Figure 1A).

In the FT-IR spectrum of HA-SH (Supplementary Figure 1B), a small peak of -SH group was observed at approximately 2550 cm^{-1}. The signal of -SH group peak was very weak and broad due to the hydrogen bonding of -SH group as also observed by other researchers [75,76]. In addition, the HA-SH derivatives exhibited to have 0.763 ± 0.016 mM (n = 3) of -SH groups as determined by Ellman's method [37]. Overall, FT-IR and NMR analyses confirmed the effective thiol modification of native HA polymer.

SEC & PXRD analyses

SEC analysis showed that the average MW of HA-SH was approximately 58 kDa which was close to the average MW of native HA (~60 kDa) (Supplementary Figure 2A). PXRD results revealed that the amorphous nature of native HA has been maintained during the reaction process (Supplementary Figure 2B). PXRD spectrum of HA-SH showed one additional peak at 2θ of 32° which was the typical PXRD peak of NaCl [77]. This could be due to the crystallization of the NaCl resulting from the sodium ions (Na^+) of HA and the chloride ions (Cl^-) of HCl used in the pH adjustment media. Overall, SEC and PXRD analysis results confirmed that the native HA was quiet stable under the thiol modification reaction process.

Formulation & physicochemical characterization of HA-SH-NFs

The synthesized HA-SH polymer was used to formulate HA-SH-NFs. During the electrospinning process, a polymer solution was injected through a needle by electrostatic repulsive forces on a grounded collector (Figure 3A) [78]. The charged fluid jet underwent a highly stretching and whipping process through the air and the solvent evaporated quickly, and as a result, NFs were formulated and deposited on the collector. Initially, the HA-SH solution was electrospun alone and no fibers were formed due to the high viscosity and enormous water affinity of HA [38]. However, the blended HA-SH and PEO solutions produced NFs since PEO facilitated the fiber formation during the electrospinning process as confirmed by the SEM images.

Surface morphology & size distribution analysis

The mean diameter of the HA-SH-NFs engineered using the electropinning process (Figure 3A) was found

to be 74.96 ± 46.31 nm (n = 100) (Figure 3D). The SEM images revealed that the blended HA-SH and PEO solutions produced the HA-SH-NFs (Figure 3B) since PEO facilitated the fiber formation process during the electrospinning process. Some beaded fibers were also observed (Figure 3C) which could be due to various factors such as the presence of ionizable groups on the HA-SH polymer, feed rate of electrospinning solutions and polymer concentrations [78]. The repulsive force between the ionizable groups within the polymer backbone limits its electrospinnability and inhibits the formation of continuous fiber under the high electric field [79].

In vitro mucoadhesion analysis

The mucoadhesive property of HA-SH-NFs to native HA was confirmed by the mucin interaction and ellipsometer measurements.

Mucin interaction assay

Mucin interaction study showed the relationship between the size of mucin and polymer aggregate was correlated to the mucoadhesive property of HA-SH-NFs to native HA. Results showed that the size of HA-SH-NFs was significantly increased to approximately 4–7 µm compared with the native HA (~1–3 µm) in the presence of mucin as analyzed after 3 h incubation in PBS (Figure 4A), VFS (Figure 4B) and water (Figure 4C). This was due to the higher thiol-thiol (S–S) group interactions between mucin and thiolated HA-SH-NFs in addition to the hydrophobic and electrostatic interactions. However, the study of mucin-HA interaction was limited due to the very large and broad size distribution of these two molecules and thus, the interaction between mucin and HA-SH-NFs needs to be further analyzed using more sophisticated microscopy methods such as atomic force microscopy in the future.

Ellipsometer measurements

In the ellipsometer measurements, an increased mucoadhesion of HA-SH-NFs was confirmed by an increase in thickness (~3-fold) (Figure 4D) and adsorbed mucin amount (~2-fold) (Figure 4E) of HA-SH-NFs (~321 nm, ~34 µg/cm^2, respectively) compared to the native HA data (~105 nm, ~19 µg/cm^2, respectively) as calculated by Equation 2.

In vitro drug release analysis of HA-SH-NFs

The *in vitro* drug release profile for TFV loaded HA-SH-NFs (loading ~16–17% w/w) in the presence and absence of HAase enzyme was depicted in Figure 3E. A significantly triggered drug release (~87%w/w) was observed from HA-SH-NFs in the presence of HAase enzyme, whereas, in its absence the value was approximately 54%w/w after 1 h. The cumulative percent drug release was approximately 99% and 62% w/w after a 6 h analysis in the presence and absence of HAase enzyme, respectively.

The observed drug release from HA-SH-NFs might be due to two facts: first, it was anticipated that the interaction between -COOH groups of the HA and amino groups of TFV could have affected the drug release profile of HA-SH-NFs. Since, TFV has two pKa values (2.0 and 6.7) [80], whereas HA has a pKa value at 2.9 [81], both (native TFV and HA) will have a negative charge at the working pH (7.2) of the release medium. Therefore, there would be a minimal possibility of interaction between TFV and HA. Due to these minimal interactions of HA with TFV, a higher % cumulative drug release was also observed from HA-SH-NFs in the absence of HAase during the first couple of hours. However, the drug release was significantly lower than that observed in the presence of HAase. Second, the large surface areas to volume ratios of HA-SH-NFs provided a larger area for drug interaction with the surrounding medium. This facilitated the mass transfer and thus, a fast release of drug was observed.

Ideally, the effective molar concentration (EC_{50}) of TFV (5–7.6 µM) [82] required to exhibit its anti-HIV activity should be locally released from HA-SH-NFs before the HIV crosses the vaginal mucosa in the time frame of 2–6 h and interacts with macrophages and dendritic cells [83]. Based on the drug loading of HA-SH-NFs (~16–17% w/w), the actual amount of TFV was approximately 59 µM per 100 mg of NFs. Considering the 10 mg of HA-SH-NFs will be used in each treatment dose, this would be equivalent to approximately 6 µM of TFV dose. Based on the drug release data observed, it can be reasonably speculated that the amount of microbicide released from HA-SH-NFs would potentially exhibit an anti-HIV effect in less than 6 h as most of the drug from HA-SH-NFs was released out (~99% w/w) within this time frame. It is noteworthy that the EC_{50} value of TFV from HA-SH-NFs was achieved within that critical time-frame of 2–6 h considering there is no significant drug leakage from nanoformulations after intravaginal administration in the presence of HAase.

The drug release profile from HA-SH-NFs was analyzed using various *in vitro* kinetic models [57,58]. The model with a higher R or R^2 values and lower AIC value was considered to be the best. It was observed that in the absence of HAase, the drug release from NFs followed the Peppas model (*R: 0.995*; *R^2: 0.990*; *AIC: 25.030*) however, in the presence of HAase, NFs followed Weibull model (*R: 0.999*; *R^2: 0.999*; *AIC: 9.396*) (Supplementary Table 1).

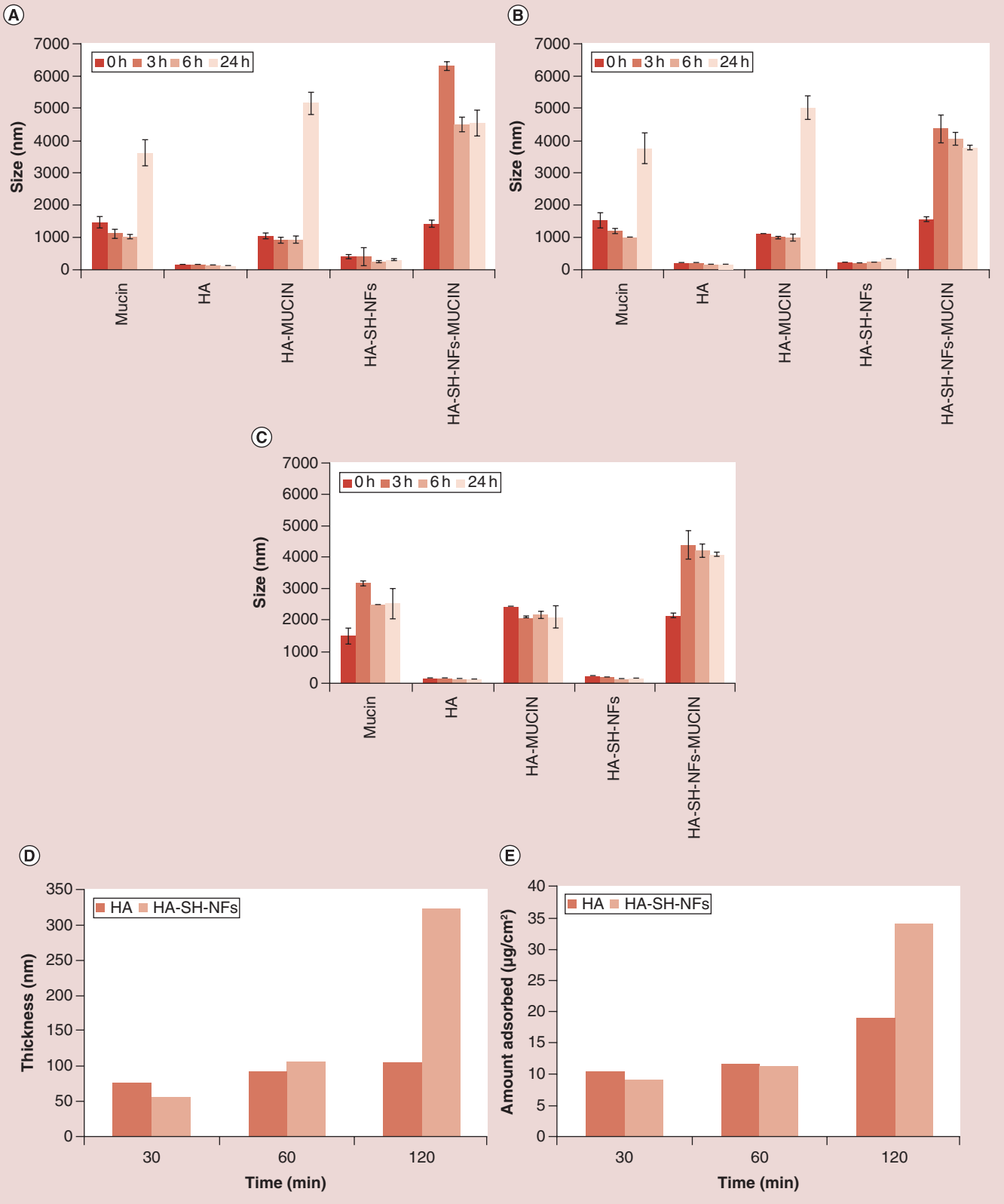

Figure 4. *In vitro* mucoadhesion analysis: mucin interaction method. (A) PBS (pH 7.4). **(B)** VFS (pH 4.2). **(C)** Water (with 10 mM NaCl). Ellipsometer measurements. **(D)** Thickness (*d*) in nm. **(E)** Amount adsorbed (*m*) in µg/cm².
HA: Hyaluronic acid; HA-SH-NF: Hyaluronic acid nanofiber; PBS: Phosphate-buffered saline; VFS: Vaginal fluid simulant.

Table 1. Vaginal and rectal tissues pharmacokinetics parameters of tenofovir in 1% hydroxyethylcellulose gel and thiolated hyaluronic acid nanofibers.

PK parameters	1% TFV-HEC gel (vagina)	HA-SH-NFs (vagina)	1% TFV-HEC gel (rectum)	HA-SH-NFs (rectum)
T_{max}	1 h	1 h	4 h	24 h
C_{max}	291.22 μg/g	561.46 μg/g	1597.06 μg/g	1715.48 μg/g
$AUC_{1–72\ h}$	14.38 mg.h/g	23.89 mg.h/g	72.50 mg.h/g	84.04 mg.h/g

HA-SH-NF: Hyaluronic acid nanofiber; PK: Pharmacokinetics; TFV-HEC: Tenofovir hydroxyethylcellulose.

In vitro cytotoxicity analysis of HA-SH-NFs

Cytotoxicity on vaginal keratinocytes cells

Cytotoxicity evaluation is an important factor in developing a topical microbicide delivery system as it should not damage the vaginal/endocervical epithelium, disturb normal vaginal flora or trigger any immune-response. According to ISO standard, if the cell viability of control samples is 100%, tested samples with a viability >80% have no cytotoxicity. Cell viability of 60–80% correspond to mild cytotoxicity, 40–60% to moderate cytotoxicity and <40%, to severe cytotoxicity [84]. Based on the results obtained, HA-SH-NFs did not show any significant effect ($p > 0.05$) on the viability of VK2/E6E7 and End1/E6E7 cells, compared with medium (negative control) (Figure 5A). A statistically insignificant ($p > 0.05$) lower LDH release and percent cytotoxicity was observed from cells incubated with HA-SH-

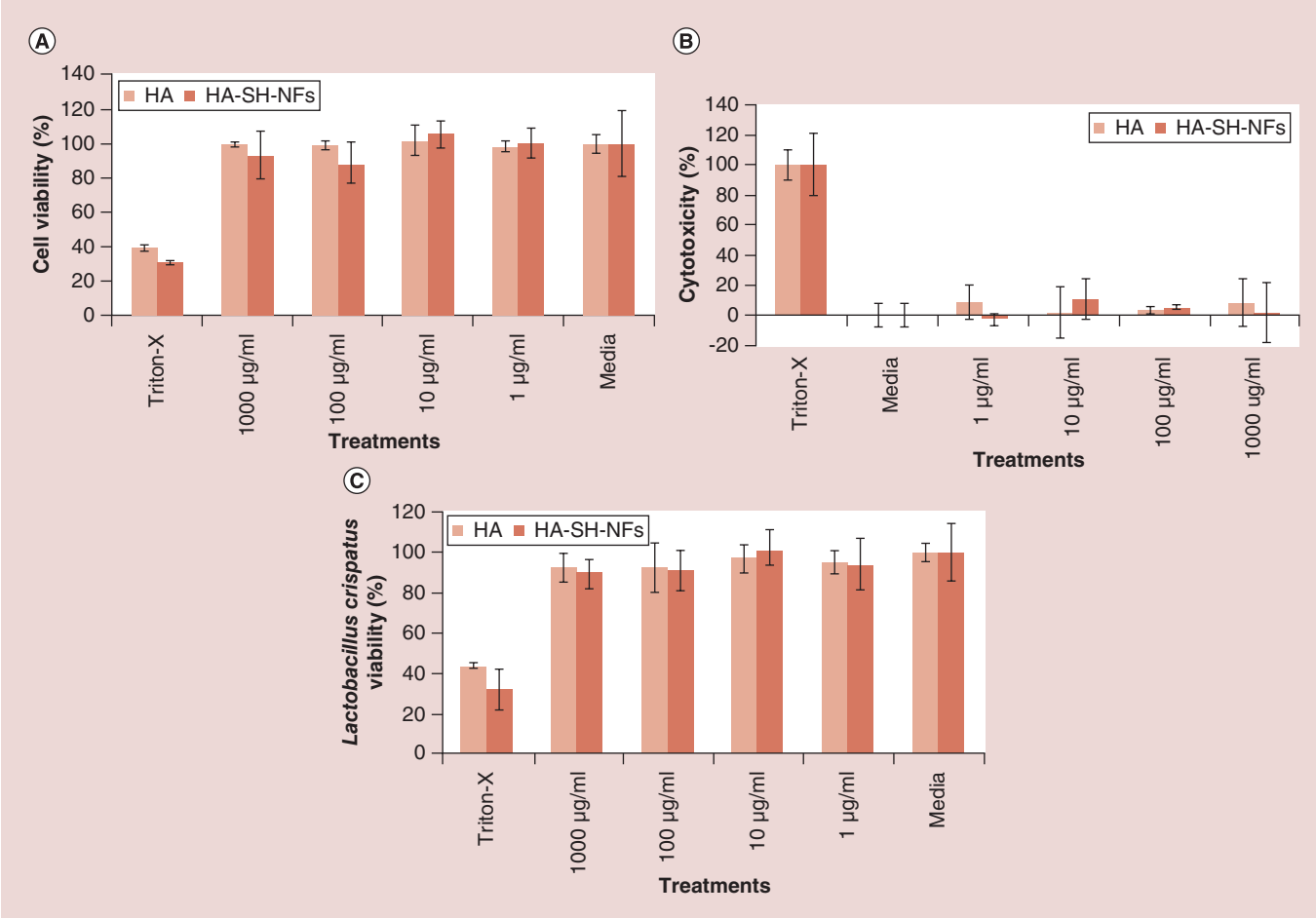

Figure 5. Cytotoxicity assays of tenofovir-loaded thiolated hyaluronic acid nanofibers. (A) Effects on the viability of VK2/E6E7 and End1/E6E7 cells (MTS assay). **(B)** Effects on lactate dehydrogenase release from VK2/E6E7 and End1/E6E7 cells (LDH assay). **(C)** Effects on the viability of *Lactobacillus crispatus* bacteria. Results are given as mean ± SD, n = 3 after 48 h incubation.
HA: Hyaluronic acid; HA-SH-NF: Hyaluronic acid nanofiber.

NFs for 48 h in comparison to the negative control (medium) (Figure 5B).

Effects on the viability of L. crispatus bacteria

A microbicide formulation should not disturb the normal *Lactobacillus* vaginal microflora since this can enhance the risk of HIV transmission through CV mucosa [59]. As shown in Figure 5C, HA-SH-NFs have no significant ($p > 0.05$) deleterious effect over the viability of *L. crispatus* bacteria compared with the negative control (medium). Overall, the cytotoxicity and *lactobacillus* viability assays of HA-SH-NFs showed that the formulation was safe to vaginal/endocervical epithelium cells.

In vivo evaluations of HA-SH-NFs

Preclinical safety plays an important role before proceeding with formulation testing in clinical trials. A microbicide formulation may elicit a transient change in the mucosal tissues, significant production and secretion of proinflammatory cytokines. This leads to the recruitment and activation of HIV-susceptible cells that could enhance HIV transmission through vaginal mucosa. The disruption of the CV epithelia can increase the HIV transmission through CV mucosa [85,86] and hence must be analyzed with any microbicide formulation.

Osmolality determination

In addition to the preclinical safety, the osmolality of a vaginal microbicide formulation could have profound effects on the vaginal environment and epithelium which could enhance HIV vaginal transmission and infection [87,88]. The normal osmolality of female vaginal secretions was reported in the range of 260–290 mOsm/kg and for human semen the value was 250–380 mOsm/kg [50,51]. Ideally, the osmolality of a microbicide formulation should not exceed 400 mOsm/Kg [63] to minimize any risk of vaginal epithelial damage. In this study, the osmolality values determined for each tested samples were well below the recommended osmolality for intravaginal application (<400 mOsm/kg) except for the N-9 (>1200 mOsm/kg). Mice were inspected daily during HA-SH-NFs treatment and no alterations in behavior, body weight or temperature was noted between the treatment and control mice groups.

Vaginal cytology analysis

The mice CVL cells were used to identify the stages of the mouse estrous cycle (proestrus, estrus, metestrus and diestrus) (Supplementary Figure 3). During the proestrus stage, clusters of round, well-formed nucleated epithelial cells (white arrow) were observed whereas, during estrus cycle, cells were predominantly cornified squamous epithelial cells (red arrow). The metestrus stage was mainly represented by the presence of small, darkly stained leukocytes (blue arrow) with some cornified squamous epithelial cells. The last stage of the estrous cycle, diestrus, was associated predominantly with leukocytes including some nucleated epithelial cells. Very few and rare cornified squamous epithelial cells may still be present. It was observed that Depo-Provera treatment maintained the diestrus conditions in the mice vagina as analyzed up to 9 days whereas, control mice (no Depo-Provera treatment) showed changes in the estrous cycle stages (appearance of the different cell types) at different days (Supplementary Figure 3).

Immunohistological assays

The histological analysis of the mice genital tract (vagina, cervix, uterus and ovary), rectum and other organs (spleen, lung, liver, kidney, heart, brain) did not show any signs of toxicity and damage upon once-daily administration of HA-SH-NFs up to 24 h (Figure 6A & B) and 7 days (Figure 6C & D). In the case of the vagina, no histological changes were observed in mice treated with HA-SH-NFs, and PBS (negative control groups). However, a clear thinning and stripping (damage) of the epithelium was observed (indicated by red arrows) following 24 h treatment in the N-9 and BZK treated mice (positive control groups) (Figure 6A) and a layer of dead cells was shown after 7 days treatment (Figure 6C). These observations further supported the toxicity of N-9 and BZK to the vaginal mucosa. For the uterus and ovary, no signs of alterations were observed in the presence of any of the tested samples including the positive controls. This suggested that N-9 and BZK were not able to reach the upper genital tract in sufficient quantities to produce any toxicity or damage.

Immunoassay of cytokines secretion in CVL

Cytokines play an important role in HIV infection and transmission through CV mucosa and must be evaluated for any microbicide formulation [89]. A microbicide formulation was supposed to be in contact with the CV epithelium for a variable time before sexual intercourse and thus, should not cause the onset of inflammation or cytokine secretions [86]. Levels (pg/ml) of different cytokines including IL-1α, IL-1β, IL-6, IL-7, IP-10, TNF-α and a chemokine (MKC) in CVL and genital tissues were analyzed after 24 h treatment with PBS (negative control), N-9 and BZK (positive controls), and HA-SH-NFs (treatment). The selection of these cytokines and MKC chemokine was based on the following facts. IL-1α and IL-1β

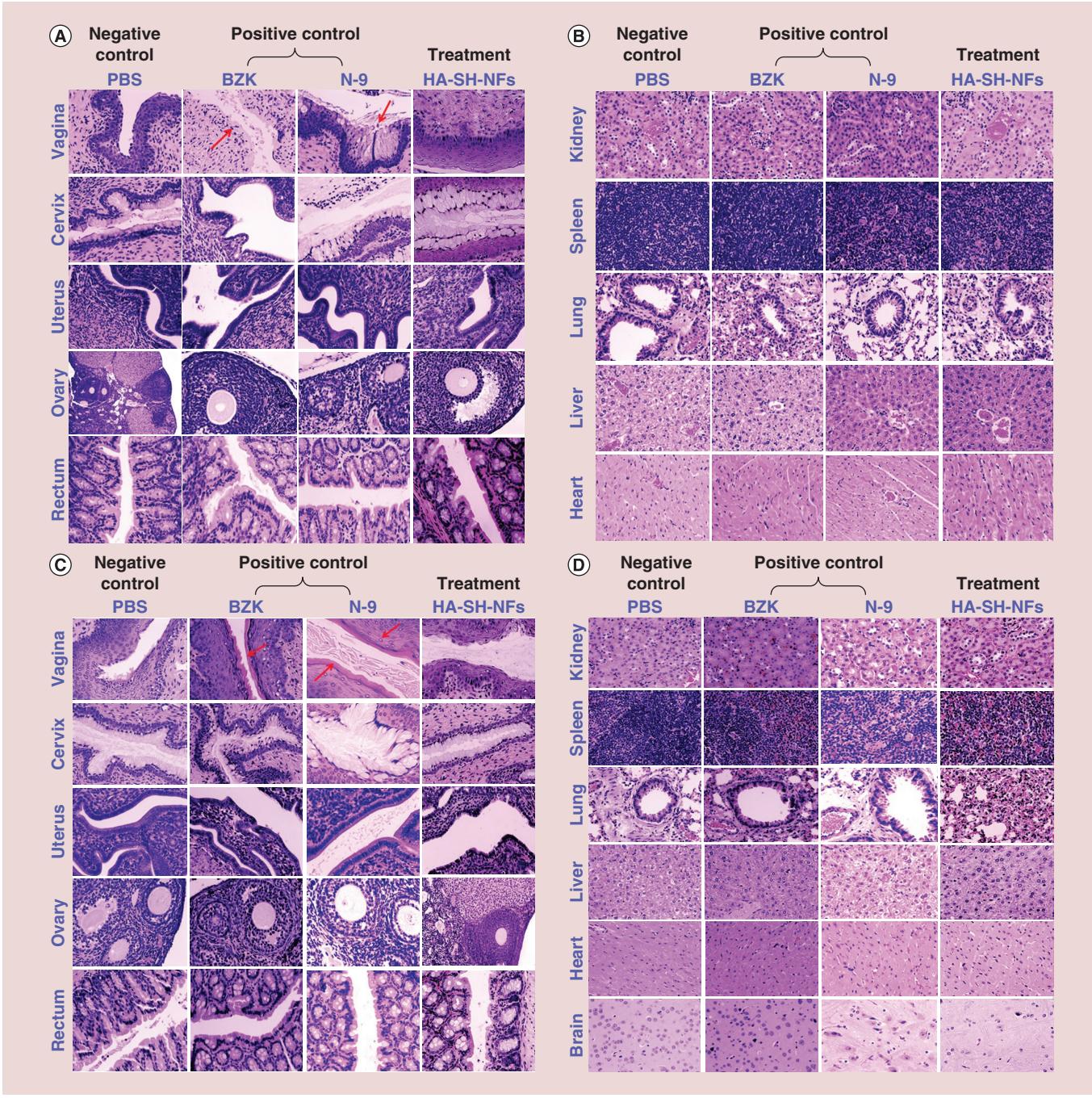

Figure 6. Preclinical safety and toxicity evaluation on female C57BL/6 mice after exposure to tenofovir loaded thiolated hyaluronic acid-nanofibers and controls. **(A)** Genital tract tissues (vagina, cervix, uterus, ovary) and, rectum after 24 h exposure. **(B)** Other tissues (kidney, spleen, lung, liver and heart) after 24 h exposure. **(C)** Genital tract tissues (vagina, cervix, uterus, ovary) and rectum after 7 days exposure. **(D)** Other tissues (kidney, spleen, lung, liver, heart and brain) after 7 days exposure. Red arrows showed the epithelial damage in tissues.
BZK: Benzalkonium chloride; HA-SH-NF: Hyaluronic acid nanofiber; N-9: Nonoxynol-9; PBS: Phosphate-buffered saline.

are efficient inducers of the proinflammatory signals, released by injured epithelial tissues and enhance the HIV replication process [59]. IL-6 enhance the HIV replication process and act as a growth factor for HIV virus. It has been recently shown that IL-7 facilitates HIV transmission to CV tissues [90]. In addition, IL-7 also promotes HIV persistence during antiretroviral treatment by enhancing residual levels of viral production and inducing the proliferation of latently infected $CD4^+$ T cells [91]. IP-10 is significantly associated with

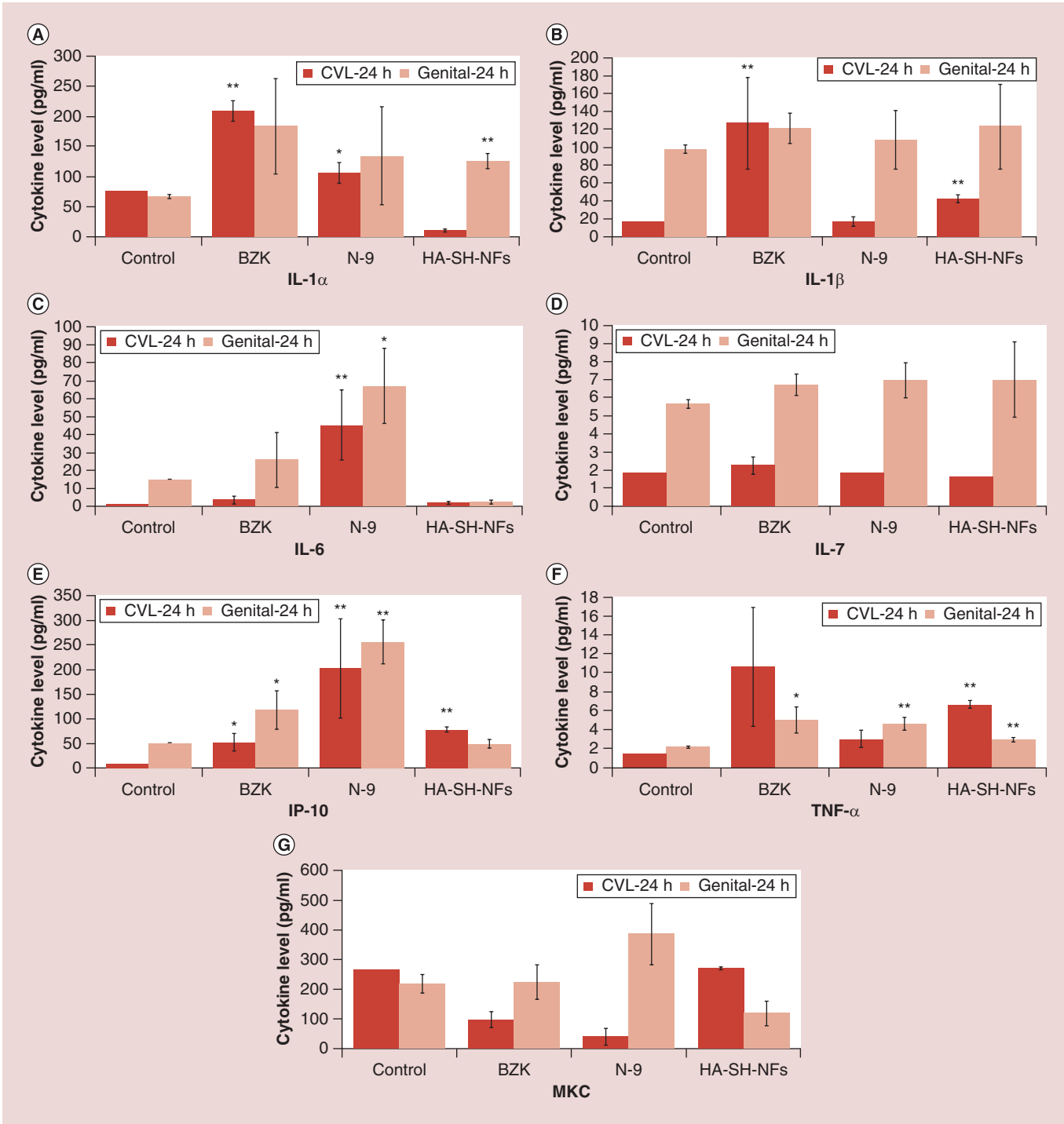

Figure 7. Cervicovaginal lavage fluid and genital tissues cytokines and chemokine levels after 24 h exposure to tenofovir-loaded thiolated hyaluronic acid nanofibers. (A–F) Data related to cytokines IL-1α, IL-1β, IL-6, IL-7, IP-10, TNF-α, respectively. **(G)** MKC chemokine levels. Results are given as mean ± SD, n = 4.
*p < 0.05; **p < 0.005.
BZK: Benzalkonium chloride; CVL: Cervicovaginal lavage; HA-SH-NF: Hyaluronic acid nanofiber; N-9: Nonoxynol-9.

high vaginal viral load and its higher level decreases the T-cell functions in HIV infected individuals on retroviral therapy [92]. MKC is a chemokine and equivalent to the human IL-8 cytokine which stimulates the HIV replication process [93]. TNF-α is one of the most important proinflammatory cytokines that induces the levels of IL-6 and IL-8 and helps in upregulation of HIV replication [59].

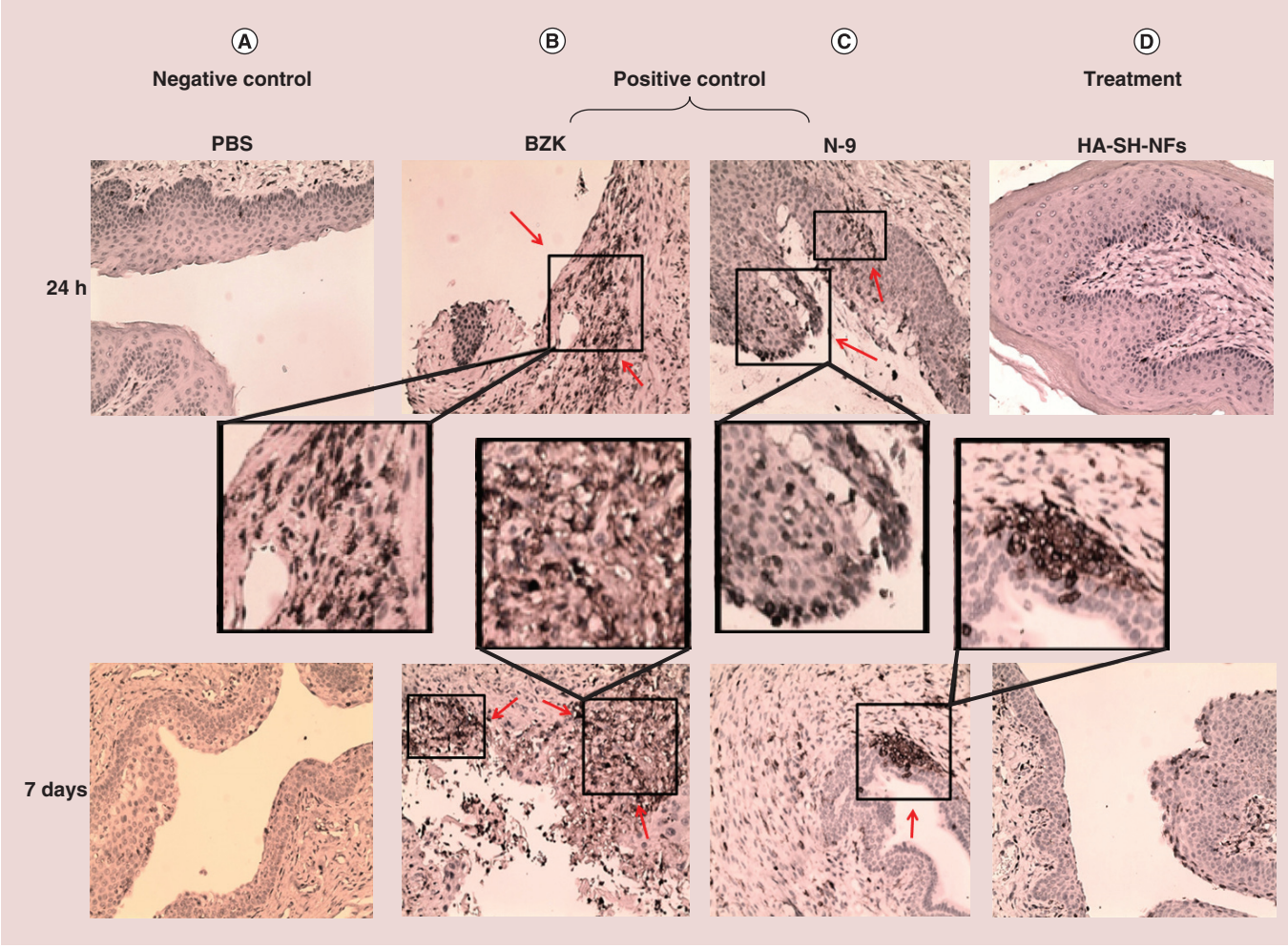

Figure 8. Immune cells (CD45) infiltration on female C57BL/6 mice vaginal tissues after 24-h and 7-day exposure to (A) negative control; (B) BZK; (C) N-9; (D) TFV-loaded thiolated HA-SH-NFs. Red arrows showed the CD45 infiltration in vaginal tissues.
BZK: Benzalkonium chloride; HA-SH-NF: Hyaluronic acid-nanofiber; N-9: Nonoxynol-9; PBS: Phosphate-buffered saline; TFV: Tenofovir.

Based on above mentioned facts and the roles of cytokines in HIV vaginal transmission, it was important to check the levels of these cytokines after a microbicide formulation application. Results showed that the levels of most of the cytokines were not significantly induced after HA-SH-NFs treatment compared with the control CVL and genital tissue samples except for the IL-1α/TNF-α in genital track tissue and IL-1β/IP-10/TNF-α in CVL (Figure 7). However, cytokines levels were well below their standard values reported [94,95].

Inflammatory cells identification in CV tissue

In addition to cytokines, an increased lymphocytes infiltration within the vagina epithelium is indicative of vaginal inflammation [61]. The CD45-associated protein is a lymphocyte-specific membrane protein and analyzed in this study. To identify the inflammatory cells (CD45) infiltration in the mice genital tract, the immunohistochemistry assay was performed. Following 24 h exposure, negative control (Figure 8A) and HA-SH-NFs (Figure 8D) treated mice tissues did not show any significant immune cell infiltration in the genital tract. Moreover, few surface and luminal lymphocytes were observed. A significant high number of immune cells infiltration was noted in BZK (Figure 8B) and N-9 (Figure 8C) treated mice (indicated by red arrows). However, very few, but not significant CD45 cells were observed after 7 days treatment with HA-SH-NFs compared with BZK or N-9 treated groups which suggested the lack of vaginal inflammation.

Overall, the cytokine and immunohistochemistry data supported that HA-SH-NFs were potentially safe for intravaginal application.

In vitro anti-HIV activity of HA-SH-NFs

Pseudotyped virus particle generation & characterization

To determine the *in vitro* anti-HIV activity of HA-

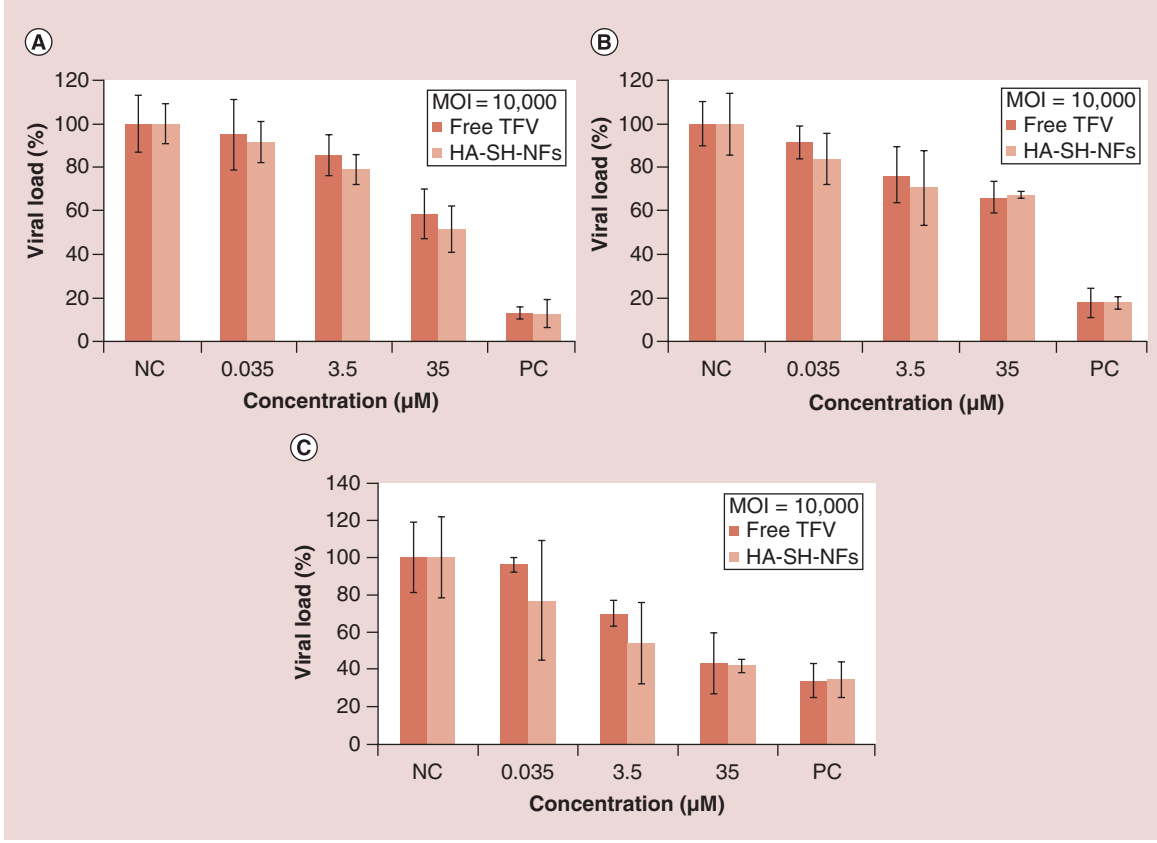

Figure 9. *In vitro* anti-HIV activity of tenofovir-loaded thiolated hyaluronic acid nanofibers on pseudotyped HIV virus particles at the MOI of (A) 10,000; (B) 5000; (C) 1000. Results are given as mean ± SD, n = 3.
HA-SH-NF: Thiolated hyaluronic acid nanofiber; MOI: Multiplicity of infection; TFV: Tenofovir.

SH-NFs, the pseudotyped HIV virus particles were generated using plasmid transfection method (Supplementary Figure 4A) and analyzed using a NTA (Supplementary Figure 4B). The mean diameter of the pseudotyped virus particles was found to be 128.00 ± 15.53 nm (n = 6) and the virus titer (number of particles/ml) was determined to be $3.07 \times 10^{10} \pm 0.30$/ml (n = 6) in cell culture media. A clear difference between the background and sample containing pseudotyped virus particles was observed (Supplementary Figure 4B) which confirmed the presence of pseudotyped virus particles.

In vitro anti-HIV activity

The *in vitro* anti-HIV activity of HA-SH-NFs on MT-4 cells at the MOI of 10,000 (Figure 9A), 5000 (Figure 9B) and 1000 (Figure 9C) at different equivalent drug concentrations showed that the NFs effectively inhibited the virus replication process. However, the effect was not different compared with that of the free drug. This was consistent with recent observations by other researchers [29]. This could be due to the fact that the cell treatment with the pseudotyped HIV virus was performed after the 24-h treatment with HA-SH-NFs and by that time, most of the encapsulated drug was released out of NFs as shown in the release profile (Figure 3E). This probably led to have an equal amount of free TFV in both HA-SH-NFs cell treated media and in the media of free TFV treated cells leading to similar level of anti-HIV activity in both cases. Future studies should be performed at different time points after HA-SH-NFs treatment in the presence and absence of HAase enzyme to determine the influence of the enzyme responsiveness of these NFs on their antiviral activity.

The *in vitro* anti-HIV activity of TFV and HA-SH-NFs was significantly increased as the MOI was lowered from 10,000 to 1000. This could be due to the presence of fewer virus particles exposed to the native TFV or HA-SH-NFs as MOI was lowered. Cytotoxicity data confirmed that the HA-SH-NFs were non-cytotoxic to MT-4 cells and produced no significant effect ($p > 0.05$) on MT-4 cells viability, compared with the medium (data not shown).

Although, the anti-HIV activity of free TFV and TFV in HA-SH-NFs was not significantly different, the *in vitro* anti-HIV activity assay results suggested that the drug maintained its structural integrity, and

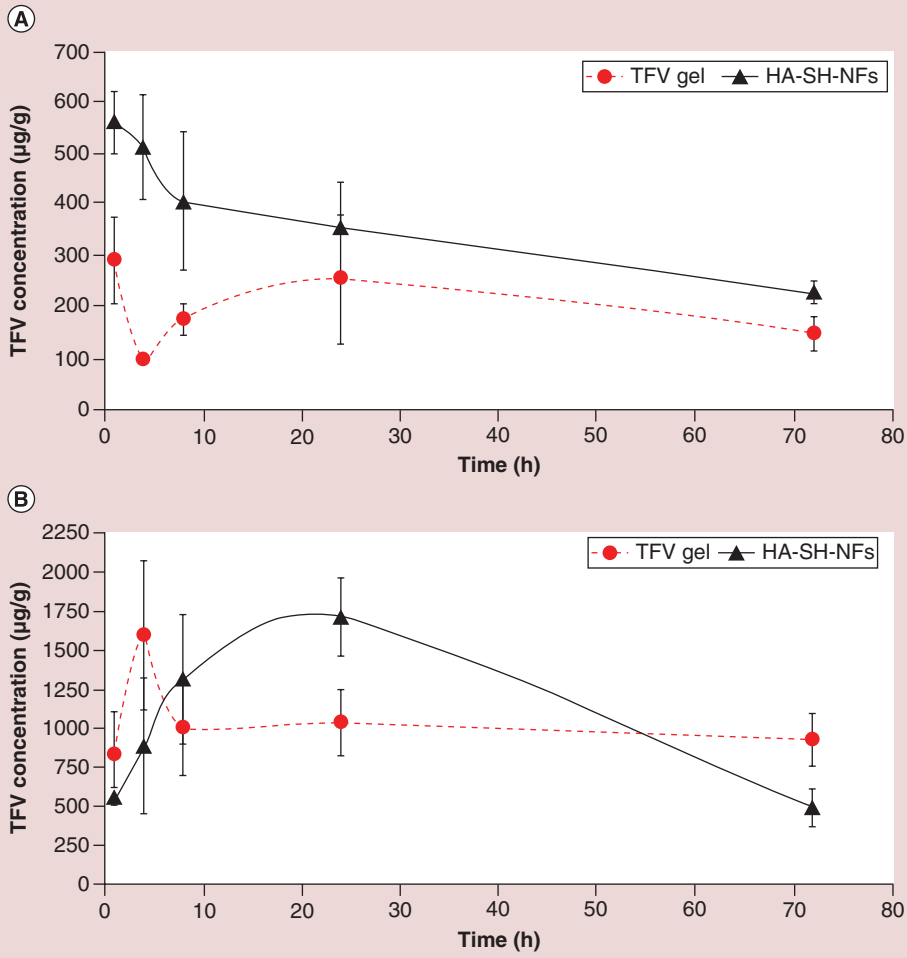

Figure 10. Pharmacokinetics profile of tenofovir. TFV levels following intravaginal administration of TFV loaded HA-SH-NFs and 1% TFV-gel in vaginal **(A)**, and rectal **(B)** tissues. Results are given as mean ± SD, n = 4.
HA-SH-NF: Thiolated hyaluronic acid-nanofiber; TFV: Tenofovir

the activity of TFV was unaffected by composite geometry of HA-SH-NFs. In addition, drug formulations such as NFs have several advantages compared with the native drug, including the ability for sustained/controlled drug release with a potential reduction in the side effects, and protection of native drug against harsh local environmental conditions (acidic pH, oxidation, degradative enzymes, etc.) in the vagina.

Tenofovir pharmacokinetic parameters in mice

TFV levels in 1% TFV-gel and HA-SH-NFs were analyzed in the mice vagina (Figure 10A) and rectal (Figure 10B & Table 1) tissues between 1 h and 24 h postadministration. TFV release profile showed that the drug transport from vagina to rectum in 1% TFV-gel occurred quickly compared with HA-SH-NFs as evidenced by the relatively low T_{max} value of 1% TFV-gel. This could be due to the immediate leakage of TFV from the vaginal cavity to the rectum because of the short genital-anal distance and the close proximity of the vaginal and rectal tissues.

Comparing the vaginal tissue TFV levels with HA-SH-NFs and TFV-gel, it was clearly observed that the HA-SH-NFs were able to increase the drug retention. In case of TFV-gel, a lower C_{max} value was observed compared with HA-SH-NFs formulation. Results have clearly shown that TFV in NFs stayed longer due to the bioadhesive and protective nature of the developed formulation. Moreover, HA-SH-NFs seem to provide a higher bioavailability of TFV in vaginal tissue as observed by higher AUC_{1-72h} value compared with the 1% TFV-gel (Table 1).

Conclusion

In this study, a novel bioresponsive, mucoadhesive and biocompatible thiolated HA-based NFs loaded with a vaginal anti-HIV microbicide TFV were developed using the electrospinning method. It was observed

that HAase enzyme triggered a significant drug release from HA-SH-NFs. HA-SH-NFs were noncytotoxic to human vaginal VK2/E6E7, and End1/E6E7 cells and had no deleterious effect on the viability of *Lactobacillus* bacteria. Histological analyses confirmed the safety of HA-SH-NFs in C57BL/6 mice genital tract and other organs. Moreover, NFs did not induce any CD45 immune cell infiltration in genital tract tissues. The cytokine levels were not significantly changed for most of the tested cytokines in CVL and CV tissues. The HA-SH-NFs were able to increase the TFV retention and provided a higher drug bioavailability in vaginal tissue, including the lower drug disposition to the rectum tissue compared with the 1% TFV-gel. The *in vitro* anti-HIV activity data showed that the drug loaded HA-SH-NFs were able to inhibit the replication process of pseudotyped HIV virus and the anti-HIV activity of TFV was preserved after the electrospinning process.

One limitation of the previously reported HAase triggered drug release from the HA based nanoparticles (HA-NPs) was the drug release time: it took about 24 h to reach approximately 90% w/w [2]. However, the release profile of HA-SH-NFs developed in this study has significantly been improved and a triggered drug release was observed after 1 h of incubation in the presence of HAase enzyme. This could be due to the absence of any cross-linking chemistry at the HAase enzyme target site (carboxylic acid groups) in HA-SH-NFs compared with that present in the HA-NPs. Moreover, the large surface areas to volume ratios and the porosity of NFs provided a larger area for drug interaction with the surrounding medium which facilitated the mass transfer and a rapid drug release.

The scalability of HA-SH-NFs fabrication method is also higher due to the involvement of fewer formulation steps compared with other TFV or microbicides formulation methods [2,23] and the availability of industrial scale nanofiber production equipments. Moreover, the method avoids toxic organic solvents and harsh acidic/alkaline formulation conditions [24–26,28,29] for sensitive bioactive agents such as protein and peptides. Further, these HA-SH-NFs have additional advantages of being mucoadhesive in nature due to the presence of thiol groups on their surface. However, further experiments are needed to confirm the proof-of-concept of this work such as: *in vivo* stimuli-responsiveness, drug release and bioretention of these nanoformulations in the presence of seminal fluid and HAase enzyme; expanding the application of HA-SH-NFs platform to other topical microbicides (fusion/entry inhibitors) alone or in combination with other reverse transcriptase inhibitors; analyzing the interaction between mucin and HA-SH-NFs using other methods such as atomic force microscopy; analyzing the *in vivo* anti-HIV efficacy of developed NFs in an appropriate animal model. Overall, the data presented here highlight the potential of HA-SH-NF templates for the vaginal delivery of anti-HIV/AIDS microbicides.

Supplementary data

To view the supplementary data that accompany this paper please visit the journal website at: www.futuremedicine.com/doi/full/10.2217/nnm-2016-0103

Acknowledgements

The content is the sole responsibility of the authors and does not necessarily represent the official views of the National Institute of Allergy and infectious Diseases or the National Institutes of Health. We are thankful to JB Murowchick (Department of Geosciences, UMKC) for his kind help in PXRD analysis and Tim Quinn (School of Medicine, UMKC) for his technical assistance in immunohistochemistry assays. We are thankful to MB Kruger and JA Crow (Department of Physics, UMKC) for allowing us to use the ellipsometer instrument and helping in taking measurements. Our sincere thanks to N Qureshi (School of Medicine, UMKC) for allowing us to use the Luminometer instrument and in bioluminescence assays. The following reagents were obtained through the NIH AIDS Research and Reference Reagent Program, Division of AIDS, NIAID, NIH: MT-4 cells from D Richman; the plasmid pNL4–3.Luc.R$^-$.E$^-$ from N Landau and pHEF-VSVG from L Chang.

Financial & competing interests disclosure

The project was supported by award number R01AI087304 from the National Institute of Allergy and Infectious Diseases (NIAID, MD, USA). The authors have no other relevant affiliations or financial involvement with any organization or entity with a financial interest in or financial conflict with the subject matter or materials discussed in the manuscript apart from those disclosed.

No writing assistance was utilized in the production of this manuscript.

Ethical conduct of research

The authors state that they have obtained appropriate institutional review board approval or have followed the principles outlined in the Declaration of Helsinki for all human or animal experimental investigations. In addition, for investigations involving human subjects, informed consent has been obtained from the participants involved.

Executive summary

Thiolated polymer synthesis & nanocarrier formulation

- Sulfhydryl (-SH) group modified thiolated-hyaluronic acid (HA) polymer (HA-SH) was synthesized and physicochemically characterized.
- Bioresponsive, mucoadhesive and biocompatible loaded HA-SH based nanofibers (HA-SH-NFs: mean diameter ~75 nm) loaded with a vaginal anti-HIV microbicide (tenofovir [TFV]) were engineered by electrospinning process.

Physicochemical characterization of nanocarrier formulation

- Mucin-interaction and ellipsometer studies confirmed the higher mucoadhesion of HA-SH-NFs compared with the native-HA polymer.
- Semen hyaluronidase (HAase) enzyme triggered drug release within 1 h from these NFS (potential clinical relevance: HIV virus vaginal occurs in approximately 2–6 h).

***In vitro* cytotoxicity of nanocarriers**

- HA-SH-NFs NFs were noncytotoxic to the human vaginal cells and *L. crispatus* bacteria.
- *In vivo* safety, biocompatibility and immuno-histochemical evaluation of nanocarriers.
- HA-SH-NFs did not induce any tissue damage on the C57BL/6 mice genital-tract and other vital organs upon once-daily administration for 7 days.
- No significant CD45 cell-infiltration and changes in cytokines levels in cervicovaginal tissues were observed following 24 h of exposure to the HA-SH-NFs.

***In vitro* anti-HIV activity of nanocarriers**

- *In vitro* anti-HIV activity data (analyzed by luciferase assay) suggested that the drug maintained its structural integrity after nanofabrication.
- HA-SH-NFs inhibited the *in vitro* replication process of pseudotyped HIV.

Pharmacokinetics & *in vivo* drug release profile of nanocarriers

- HA-SH-NFs significantly increased the TFV retention and bioavailability in vaginal tissue compared with the 1% TFV-gel.

Conclusion & future perspective

- HA-SH-NFs could potentially serve as a safe and effective nanotemplate for topical delivery of bioactive agents such as HIV/AIDS microbicides.

References

Papers of special note have been highlighted as: • of interest; •• of considerable interest

1 Granich R, Gupta S, Hersh B *et al.* Trends in AIDS deaths, new infections and ART coverage in the Top 30 countries with the highest AIDS mortality burden; 1990–2013. *PLoS ONE* 10(7), e0131353 (2015).

2 Agrahari V, Zhang C, Zhang T *et al.* Hyaluronidase-sensitive nanoparticle templates for triggered release of HIV/AIDS microbicide *in vitro*. *AAPS J.* 16(2), 181–193 (2014).

•• **Discussed the hyaluronidase enzyme sensitive approach for vaginal microbicide delivery.**

3 Sanchez-Rodriguez J, Vacas-Cordoba E, Gomez R, De La Mata FJ, Munoz-Fernandez MA. Nanotech-derived topical microbicides for HIV prevention: the road to clinical development. *Antiviral Res.* 113, 33–48 (2015).

4 Vanic Z, Skalko-Basnet N. Nanopharmaceuticals for improved topical vaginal therapy: can they deliver? *Eur. J. Pharm. Sci.* 50(1), 29–41 (2013).

5 Valenta C. The use of mucoadhesive polymers in vaginal delivery. *Adv. Drug. Deliv. Rev.* 57(11), 1692–1712 (2005).

6 Oh EJ, Park K, Kim KS *et al.* Target specific and long-acting delivery of protein, peptide, and nucleotide therapeutics using hyaluronic acid derivatives. *J. Control. Release* 141(1), 2–12 (2010).

• **Provided an overview on novel HA derivatives and the latest advances in HA-based drug delivery systems of various biopharmaceutical applications.**

7 Mizrahy S, Raz SR, Hasgaard M *et al.* Hyaluronan-coated nanoparticles: the influence of the molecular weight on CD44-hyaluronan interactions and on the immune response. *J. Control. Release* 156(2), 231–238 (2011).

8 Jhan HJ, Liu JJ, Chen YC, Liu DZ, Sheu MT, Ho HO. Novel injectable thermosensitive hydrogels for delivering hyaluronic acid-doxorubicin nanocomplexes to locally treat tumors. *Nanomedicine (Lond.)* 10(8), 1263–1274 (2015).

9 Urbiola K, Sanmartin C, Blanco-Fernandez L, Tros De Ilarduya C. Efficient targeted gene delivery by a novel PAMAM/DNA dendriplex coated with hyaluronic acid. *Nanomedicine (Lond.)* 9(18), 2787–2801 (2014).

10 Jung HS, Kim KS, Yun SH, Hahn SK. Enhancing the transdermal penetration of nanoconstructs: could hyaluronic acid be the key? *Nanomedicine (Lond.)* 9(6), 743–745 (2014).

11 Youm I, Agrahari V, Murowchick JB, Youan BB. Uptake and cytotoxicity of docetaxel-loaded hyaluronic acid-grafted oily core nanocapsules in MDA-MB 231 cancer cells. *Pharm. Res.* 31(9), 2439–2452 (2014).

12 Sandri G, Rossi S, Ferrari F, Bonferoni MC, Zerrouk N, Caramella C. Mucoadhesive and penetration enhancement properties of three grades of hyaluronic acid using porcine

buccal and vaginal tissue, Caco-2 cell lines, and rat jejunum. *J. Pharm. Pharmacol.* 56(9), 1083–1090 (2004).

13 Leitner VM, Walker GF, Bernkop-Schnurch A. Thiolated polymers: evidence for the formation of disulphide bonds with mucus glycoproteins. *Eur. J. Pharm. Biopharm.* 56(2), 207–214 (2003).

14 Abdool Karim Q, Abdool Karim SS, Frohlich JA *et al.* Effectiveness and safety of tenofovir gel, an antiretroviral microbicide, for the prevention of HIV infection in women. *Science* 329(5996), 1168–1174 (2010).

•• **Assessed the effectiveness and safety of a 1% vaginal gel formulation of tenofovir for the prevention of HIV acquisition in women.**

15 Das Neves J, Nunes R, Rodrigues F, Sarmento B. Nanomedicine in the development of anti-HIV microbicides. *Adv. Drug Deliv. Rev.* 103, 57–75 (2016).

16 Sill TJ, Von Recum HA. Electrospinning: applications in drug delivery and tissue engineering. *Biomaterials* 29(13), 1989–2006 (2008).

17 Nista SV, Bettini J, Mei LH. Coaxial nanofibers of chitosan-alginate-PEO polycomplex obtained by electrospinning. *Carbohydr. Polym.* 127, 222–228 (2015).

18 Blakney AK, Ball C, Krogstad EA, Woodrow KA. Electrospun fibers for vaginal anti-HIV drug delivery. *Antiviral Res.* 100(Suppl.), S9–S16 (2013).

19 Tseng YY, Liu SJ. Nanofibers used for the delivery of analgesics. *Nanomedicine (Lond.)* 10(11), 1785–1800 (2015).

20 Agrahari V, Youan BB. Sensitive and rapid HPLC quantification of tenofovir from hyaluronic acid-based nanomedicine. *AAPS PharmSciTech* 13(1), 202–210 (2012).

21 Dezzutti CS, Shetler C, Mahalingam A *et al.* Safety and efficacy of tenofovir/IQP-0528 combination gels – a dual compartment microbicide for HIV-1 prevention. *Antiviral Res.* 96(2), 221–225 (2012).

22 Saxena BB, Han YA, Fu D *et al.* Sustained release of microbicides by newly engineered vaginal rings. *AIDS* 23(8), 917–922 (2009).

23 Alukda D, Sturgis T, Youan BB. Formulation of tenofovir-loaded functionalized solid lipid nanoparticles intended for HIV prevention. *J. Pharm. Sci.* 100(8), 3345–3356 (2011).

24 Meng J, Sturgis TF, Youan BB. Engineering tenofovir loaded chitosan nanoparticles to maximize microbicide mucoadhesion. *Eur. J. Pharm. Sci.* 44(1–2), 57–67 (2011).

25 Meng J, Zhang T, Agrahari V, Ezoulin MJ, Youan BB. Comparative biophysical properties of tenofovir-loaded, thiolated and nonthiolated chitosan nanoparticles intended for HIV prevention. *Nanomedicine (Lond.)* 9(11), 1595–1612 (2014).

• **Assessed the biophysical properties of tenofovir-loaded chitosan-thioglycolic acid-conjugated nanoparticles intended for the prevention of HIV transmission.**

26 Zhang T, Sturgis TF, Youan BB. pH-responsive nanoparticles releasing tenofovir intended for the prevention of HIV transmission. *Eur. J. Pharm. Biopharm.* 79(3), 526–536 (2011).

27 Zhang T, Zhang C, Agrahari V, Murowchick JB, Oyler NA, Youan BB. Spray drying tenofovir loaded mucoadhesive and pH-sensitive microspheres intended for HIV prevention. *Antiviral Res.* 97(3), 34–46 (2012).

28 Huang C, Soenen SJ, Van Gulck E *et al.* Electrospun cellulose acetate phthalate fibers for semen induced anti-HIV vaginal drug delivery. *Biomaterials* 33(3), 962–969 (2012).

29 Blakney AK, Krogstad EA, Jiang YH, Woodrow KA. Delivery of multipurpose prevention drug combinations from electrospun nanofibers using composite microarchitectures. *Int. J. Nanomedicine* 9, 2967–2978 (2014).

30 Schanté CE, Zubera G, Herlin C, Vandamme TF. Chemical modifications of hyaluronic acid for the synthesis of derivatives for a broad range of biomedical applications. *Carbohydr. Polym.* 85, 469–489 (2011).

•• **Reviewed various chemical modification methods and synthetic routes to obtain HA derivatives.**

31 Swyer GI. The hyaluronidase content of semen. *Biochem. J.* 41(3), 409–413 (1947).

32 Abdul-Aziz M, Maclusky NJ, Bhavnani BR, Casper RF. Hyaluronidase activity in human semen: correlation with fertilization *in vitro*. *Fertil. Steril.* 64(6), 1147–1153 (1995).

33 Reese KL, Aravindan RG, Griffiths GS *et al.* Acidic hyaluronidase activity is present in mouse sperm and is reduced in the absence of SPAM1: evidence for a role for hyaluronidase 3 in mouse and human sperm. *Mol. Reprod. Dev.* 77(9), 759–772 (2010).

34 Stern R, Kogan G, Jedrzejas MJ, Soltes L. The many ways to cleave hyaluronan. *Biotechnol. Adv.* 25(6), 537–557 (2007).

35 Sabatte J, Remes Lenicov F, Cabrini M *et al.* The role of semen in sexual transmission of HIV: beyond a carrier for virus particles. *Microbes. Infect.* 13(12–13), 977–982 (2011).

• **Discussed the role of semen in HIV vaginal transmission.**

36 Serban MA, Yang G, Prestwich GD. Synthesis, characterization and chondroprotective properties of a hyaluronan thioethyl ether derivative. *Biomaterials* 29(10), 1388–1399 (2008).

37 Ellman GL. Tissue sulfhydryl groups. *Arch. Biochem. Biophys.* 82(1), 70–77 (1959).

38 Liang D, Hsiao BS, Chu B. Functional electrospun nanofibrous scaffolds for biomedical applications. *Adv. Drug Deliv. Rev.* 59(14), 1392–1412 (2007).

39 Ji Y, Ghosh K, Shu XZ *et al.* Electrospun three-dimensional hyaluronic acid nanofibrous scaffolds. *Biomaterials* 27(20), 3782–3792 (2006).

40 Ji Y, Ghosh K, Li B, Sokolov JC, Clark RA, Rafailovich MH. Dual-syringe reactive electrospinning of cross-linked hyaluronic acid hydrogel nanofibers for tissue engineering applications. *Macromol. Biosci.* 6(10), 811–817 (2006).

41 Bhattarai N, Edmondson D, Veiseh O, Matsen FA, Zhang M. Electrospun chitosan-based nanofibers and their cellular compatibility. *Biomaterials* 26(31), 6176–6184 (2005).

42 Hu X, Liu S, Zhou G, Huang Y, Xie Z, Jing X. Electrospinning of polymeric nanofibers for drug delivery applications. *J. Control. Release* 185, 12–21 (2014).

43 Zamani M, Prabhakaran MP, Ramakrishna S. Advances in drug delivery via electrospun and electrosprayed nanomaterials. *Int. J. Nanomedicine* 8, 2997–3017 (2013).

44 Agrahari V, Putty S, Mathes C, Murowchick JB, Youan BB. Evaluation of degradation kinetics and physicochemical stability of tenofovir. *Drug Test. Anal.* 7(3), 207–213 (2015).

45 Takeuchi H, Thongborisute J, Matsui Y, Sugihara H, Yamamoto H, Kawashima Y. Novel mucoadhesion tests for polymers and polymer-coated particles to design optimal mucoadhesive drug delivery systems. *Adv. Drug Deliv. Rev.* 57(11), 1583–1594 (2005).

46 Das Neves J, Rocha CM, Goncalves MP *et al.* Interactions of microbicide nanoparticles with a simulated vaginal fluid. *Mol. Pharm.* 9(11), 3347–3356 (2012).

47 Svensson O, Thuresson K, Arnebrant T. Interactions between drug delivery particles and mucin in solution and at interfaces. *Langmuir* 24(6), 2573–2579 (2008).

48 Svensson O, Thuresson K, Arnebrant T. Interactions between chitosan-modified particles and mucin-coated surfaces. *J. Colloid Interface Sci.* 325(2), 346–350 (2008).

49 Ivarsson D, Wahlgren M. Comparison of *in vitro* methods of measuring mucoadhesion: ellipsometry, tensile strength and rheological measurements. *Colloids Surf. B. Biointerfaces* 92, 353–359 (2012).

50 Owen DH, Katz DF. A review of the physical and chemical properties of human semen and the formulation of a semen simulant. *J. Androl.* 26(4), 459–469 (2005).

51 Owen DH, Katz DF. A vaginal fluid simulant. *Contraception* 59(2), 91–95 (1999).

52 Svensson O. *Interactions of Mucins with Biopolymers and Drug Delivery Particles [PhD Thesis]*. Malmö University, MalmöSweden (2008).

53 Lindh L, Glantz P-O, Carlstedt I, Wickstro C, Arnebrant T. Adsorption of MUC5B and the role of mucins in early salivary film formation. *Colloids Surf. B. Biointerfaces* 25, 139–146 (2002).

54 Schmohl A, Khan A, Hess P. Functionalization of oxidized silicon surfaces with methyl groups and their characterization. *Superlattices Microst.* 36, 113–121 (2004).

55 George JP, Smet PF, Botterman J *et al.* Lanthanide-assisted deposition of strongly electro-optic PZT thin films on silicon: toward integrated active nanophotonic devices. *ACS Appl. Mater. Interfaces* 7(24), 13350–13359 (2015).

56 Theisen A, Johann C, Deacon MP, Harding SE. *Refractive Increment Data-Book for Polymer and Biomolecular Scientists*. Nottingham University Press, Nottingham, UK (2000).

57 Costa P, Sousa Lobo JM. Modeling and comparison of dissolution profiles. *Eur. J. Pharm. Sci.* 13(2), 123–133 (2001).

58 Zhang Y, Huo M, Zhou J *et al.* DDSolver: an add-in program for modeling and comparison of drug dissolution profiles. *AAPS J.* 12(3), 263–271 (2010).

59 Petrova MI, Van Den Broek M, Balzarini J, Vanderleyden J, Lebeer S. Vaginal microbiota and its role in HIV transmission and infection. *FEMS Microbiol. Rev.* 37(5), 762–792 (2013).

60 Moncla BJ, Pryke K, Rohan LC, Yang H. Testing of viscous anti-HIV microbicides using *Lactobacillus*. *J. Microbiol. Methods* 88(2), 292–296 (2012).

61 Catalone BJ, Kish-Catalone TM, Budgeon LR *et al.* Mouse model of cervicovaginal toxicity and inflammation for preclinical evaluation of topical vaginal microbicides. *Antimicrob. Agents Chemother.* 48(5), 1837–1847 (2004).

62 McLean AC, Valenzuela N, Fai S, Bennett SA. Performing vaginal lavage, crystal violet staining, and vaginal cytological evaluation for mouse estrous cycle staging identification. *J. Vis. Exp.* 67, e4389 (2012).

63 Ham AS, Nugent ST, Peters JJ *et al.* The rational design and development of a dual chamber vaginal/rectal microbicide gel formulation for HIV prevention. *Antiviral Res.* 120, 153–164 (2015).

64 Garcia JM, Gao A, He PL *et al.* High-throughput screening using pseudotyped lentiviral particles: a strategy for the identification of HIV-1 inhibitors in a cell-based assay. *Antiviral Res.* 81(3), 239–247 (2009).

65 Naldini L, Blomer U, Gallay P *et al. In vivo* gene delivery and stable transduction of nondividing cells by a lentiviral vector. *Science* 272(5259), 263–267 (1996).

66 Young J, Tang Z, Yu Q, Yu D, Wu Y. Selective killing of HIV-1-positive macrophages and T cells by the Rev-dependent lentivirus carrying anthrolysin O from *Bacillus anthracis*. *Retrovirology* 5, 36 (2008).

67 Filipe V, Hawe A, Jiskoot W. Critical evaluation of nanoparticle tracking analysis (NTA) by NanoSight for the measurement of nanoparticles and protein aggregates. *Pharm. Res.* 27(5), 796–810 (2010).

•• **Evaluated the nanoparticle tracking analysis technique and its performance in characterizing drug delivery nanoparticles and virus particles.**

68 Kramberger P, Ciringer M, Strancar A, Peterka M. Evaluation of nanoparticle tracking analysis for total virus particle determination. *Virol. J.* 9, 265 (2012).

69 Zhong P, Agosto LM, Ilinskaya A *et al.* Cell-to-cell transmission can overcome multiple donor and target cell barriers imposed on cell-free HIV. *PLoS ONE* 8(1), e53138 (2013).

70 Ivetac A, Swift SE, Boyer PL *et al.* Discovery of novel inhibitors of HIV-1 reverse transcriptase through virtual screening of experimental and theoretical ensembles. *Chem. Biol. Drug Des.* 83(5), 521–531 (2014).

71 Reagan-Shaw S, Nihal M, Ahmad N. Dose translation from animal to human studies revisited. *FASEB J.* 22(3), 659–661 (2008).

72 Guo J, Meng F, Li L, Zhong B, Zhao Y. Development and validation of an LC/MS/MS method for the determination of tenofovir in monkey plasma. *Biol. Pharm. Bull.* 34(6), 877–882 (2011).

73 Zhang Y, Huo M, Zhou J, Xie S. PKSolver: an add-in program for pharmacokinetic and pharmacodynamic data analysis in Microsoft Excel. *Comput. Methods Programs. Biomed.* 99(3), 306–314 (2010).

74 Choi KY, Min KH, Yoon HY *et al.* PEGylation of hyaluronic acid nanoparticles improves tumor targetability *in vivo*. *Biomaterials* 32(7), 1880–1889 (2011).

75 Li X, Yu G, Jin K, Yin Z. Hyaluronic acid L-cysteine conjugate exhibits controlled-release potential for mucoadhesive drug delivery. *Pharmazie* 67(3), 224–228 (2012).

76 Yadav S, Ahuja M, Kumar A, Kaur H. Gellan-thioglycolic acid conjugate: synthesis, characterization and evaluation as mucoadhesive polymer. *Carbohydr. Polym.* 99, 601–607 (2014).

77 Tu Luan, Lijiao Wu, Hongbin Zhang, Wang Y. A study on the nature of intermolecular links in the cryotropic weak gels of hyaluronan. *Carbohydr. Polym.* 87, 2076–2085 (2012).

78 Bhardwaj N, Kundu SC. Electrospinning: a fascinating fiber fabrication technique. *Biotechnol. Adv.* 28(3), 325–347 (2010).

79 Mckee MG, Wilkes GL, Colby RH, Long TE. Correlations of solution rheology with electrospun fiber formation of linear and branched polyesters. *Macromolecules* 37(5), 1760–1767 (2004).

80 Choi SU, Bui T, Ho RJ. pH-dependent interactions of indinavir and lipids in nanoparticles and their ability to entrap a solute. *J. Pharm. Sci.* 97(2), 931–943 (2008).

81 Lenormand H, Vincent JC. pH effects on the hyaluronan hydrolysis catalysed by hyaluronidase in the presence of proteins: Part II. The electrostatic hyaluronan – Protein complexes. *Carbohydr. Polym.* 85, 303–311 (2011).

82 Ferir G, Vermeire K, Huskens D *et al.* Synergistic *in vitro* anti-HIV type 1 activity of tenofovir with carbohydrate-binding agents (CBAs). *Antiviral Res.* 90(3), 200–204 (2011).

83 Haynes BF, Shattock RJ. Critical issues in mucosal immunity for HIV-1 vaccine development. *J. Allergy. Clin. Immunol.* 122(1), 3–9; quiz 10–11 (2008).

84 Rat P, Korwin-Zmijowska C, Warnet JM, Adolphe M. New *in vitro* fluorimetric microtitration assays for toxicological screening of drugs. *Cell Biol. Toxicol.* 10(5–6), 329–337 (1994).

85 Mesquita PM, Cheshenko N, Wilson SS *et al.* Disruption of tight junctions by cellulose sulfate facilitates HIV infection: model of microbicide safety. *J. Infect. Dis.* 200(4), 599–608 (2009).

86 Shattock RJ, Moore JP. Inhibiting sexual transmission of HIV-1 infection. *Nat. Rev. Microbiol.* 1(1), 25–34 (2003).

87 Adriaens E, Remon JP. Mucosal irritation potential of personal lubricants relates to product osmolality as detected by the slug mucosal irritation assay. *Sex. Transm. Dis.* 35(5), 512–516 (2008).

88 Fuchs EJ, Lee LA, Torbenson MS *et al.* Hyperosmolar sexual lubricant causes epithelial damage in the distal colon: potential implication for HIV transmission. *J. Infect. Dis.* 195(5), 703–710 (2007).

89 Connolly NC, Riddler SA, Rinaldo CR. Proinflammatory cytokines in HIV disease-a review and rationale for new therapeutic approaches. *AIDS Rev.* 7(3), 168–180 (2005).

90 Introini A, Vanpouille C, Lisco A, Grivel JC, Margolis L. Interleukin-7 facilitates HIV-1 transmission to cervico-vaginal tissue *ex vivo*. *PLoS Pathog.* 9(2), e1003148 (2013).

91 Vandergeeten C, Fromentin R, Dafonseca S *et al.* Interleukin-7 promotes HIV persistence during antiretroviral therapy. *Blood* 121(21), 4321–4329 (2013).

92 Blish CA, Mcclelland RS, Richardson BA *et al.* Genital inflammation predicts HIV-1 shedding independent of plasma viral load and systemic inflammation. *J. Acquir. Immune. Defic. Syndr.* 61(4), 436–440 (2012).

93 Das Neves J, Araujo F, Andrade F, Amiji M, Bahia MF, Sarmento B. Biodistribution and pharmacokinetics of dapivirine-loaded nanoparticles after vaginal delivery in mice. *Pharm. Res.* 31(7), 1834–1845 (2014).

•• **Assessed the potential of dapivirine loaded polymeric nanoparticles to affect the genital distribution, preclinical safety and local/systemic pharmacokinetics after vaginal delivery.**

94 Darville T, Andrews CW Jr., Sikes JD, Fraley PL, Rank RG. Early local cytokine profiles in strains of mice with different outcomes from chlamydial genital tract infection. *Infect. Immun.* 69(6), 3556–3561 (2001).

95 Packiam M, Veit SJ, Anderson DJ, Ingalls RR, Jerse AE. Mouse strain-dependent differences in susceptibility to Neisseria gonorrhoeae infection and induction of innate immune responses. *Infect. Immun.* 78(1), 433–440 (2010).